Validation Of Tissue Oxygen Saturation Determined By Near-Infrared Spectroscopy In Canine Models Of Hypoxemia And Hemorrhagic Shock

Noah D. Pavlisko

Thesis submitted to the faculty of the Virginia Polytechnic Institute and State University in partial fulfillment of the requirements for the degree of

Master of Science
In
Biomedical and Veterinary Sciences

Piedad Henao-Guerrero, Chair

Carolina Riccó

Maria Killos

August 13, 2014

Blacksburg, VA

Keywords: Canine, Hypoxemia, Hemorrhagic Shock, Tissue Oxygen Saturation, Near Infrared Spectroscopy, Oxygen delivery

Validation Of Tissue Oxygen Saturation Determined By Near-Infrared Spectroscopy In Canine Models Of Hypoxemia And Hemorrhagic Shock

Noah D. Pavlisko

ABSTRACT

The objective of this study was to evaluate the relationship between tissue oxygen saturation (StO_2) and oxygen delivery index (DO_2I). Oxygen delivery index is product of two factors arterial oxygen content (CaO_2) and cardiac index (CI). In this study the relationship between DO_2I and StO_2 was evaluated by manipulating both of these factors independently. In phase one of the study, CaO_2 was altered by manipulating the fractional inspired oxygen (FiO_2) concentration. Anesthetized dogs were evaluated at both high (0.40 and 0.95) and low (0.15 and 0.10) FiO_2 sequences. In phase two of the study, CI was altered by manipulating the volemic state. Anesthetized dogs were evaluated at hypovolemic, normovolemic and hypervolemic states. In each phase dogs were instrumented for thermodilution cardiac index (CI) and sartorius muscle StO_2. Data collected included hemoglobin concentration, heart rate (HR), MAP, CI, StO_2. Arterial oxygen content and DO_2I were calculated at each time point. Data analysis included Pearson's correlation and mixed model ANOVA ($p < 0.05$). In both phases one ($r = 0.97$; $p = 0.0013$) and two ($r = 0.97$; $p = 0.005$) there was a strong correlation between StO_2 and DO_2I. Under the conditions of this study, there was a strong correlation between StO_2 and DO_2I, suggesting that StO_2 may be used to estimate the adequacy of oxygen delivery in dogs.

ACKNOWLEDGMENTS

I would like to thank my committee members, Dr. Maria Killos, Dr. Natalia Guerrero, and Dr. Carolina Ricco for their contributions to this project. I would also like to thank my co-investigator Dr. Stephen Werre for his guidance in the statistical analysis for the project. I would like to recognize Dana Calicott for her technical assistance and the husbandry staff that cared for the dogs during the duration of the project. Finally, funding was provided by the VMRCVM Internal Research Competition Intramural Grant.

TABLE OF CONTENTS

LIST OF FIGURES AND LEGENDS

LIST OF TABLES

Chapter IV

Chapter I: Introduction

Oxygen is a key component in the oxidative reactions that drive cell metabolism and therefore is essential to survival. For multi-cellular organisms whose physical boundaries exceed the time-distance constraints of diffusion, circulatory systems have evolved to deliver oxygen to tissues remote to the gas exchange surface. Under normal physiologic conditions the rate of oxygen delivery (DO_2) greatly exceeds the rate of oxygen consumption (VO_2) in these tissues. However, under certain pathologic conditions DO_2 may become sufficiently diminished so that VO_2 becomes linearly dependent on DO_2 (Cilley et al, 1991). A decrease in DO_2 reflects a change in one of the three components of oxygen delivery; hemoglobin concentration, arterial oxygen content, and cardiac output. Once a linear relationship develops between VO_2 and DO_2, oxygen delivery becomes inadequate to maintain aerobic respiration and cellular metabolism transitions to anaerobic metabolism. The point at which this transition occurs is the critical oxygen delivery (DO_{2Crit}) (Cilley et al, 1991; Cain et al, 2007). Below this critical level cellular dysfunction and organ failure begin to develop, ultimately leading to death if not corrected.

It has been suggested that restoration of DO_2 before organ failure begins to develop will prevent further organ dysfunction and reduce mortality in patients with compromised organ perfusion (Pinsky et al, 2007). As a result, perfusion monitoring in critically ill patients is rapidly becoming a standard of care in human medicine. Traditional non-invasive methods for indirectly monitoring oxygen delivery have focused on indices of end organ function; blood pressure, urine output, and mental status changes. Although

effective at identifying states of profound hypoperfusion, occult hypoperfusion may go undetected in some patients (Scalea at al, 1994; Abou-Khalil et al, 1994). Lactate and base deficit are commonly used in intensive care units (ICU) to identify hypoperfusion in critically ill and injured patients. However, changes in lactate and base deficit require time to manifest and do not reflect instantaneous changes in perfusion status (Crookes et al, 2004). Additionally, lactate levels can be falsely elevated in patients with insufficient hepatic clearance (Wool et al, 1979). The advent of the pulmonary artery catheter (Swan-Ganz) has allowed for continuous monitoring of DO_2 in critically ill patients. Nevertheless, this technology is highly invasive, associated with a range of complications, cost prohibitive, and it is not easily deployable in an emergency (Evans et al, 2009).

Near-infrared spectroscopy (NIRS) has been developed out of a need for a more precise, responsive, minimally invasive monitor to assess tissue perfusion. NIRS exploits the differential absorption properties of deoxygenated and oxygenated hemoglobin in order to determine the ratio of oxygenated hemoglobin to total hemoglobin in the skeletal muscle. Based on this ratio, tissue hemoglobin saturation is calculated and reported as a percentage. In both animal and human clinical studies, hemoglobin saturation in the muscle has proved to be a good surrogate for global tissue perfusion (Putnam et al, 2007; McKinley et al, 2000). This is likely attributable to peripheral tissues being the first to reflect hypoperfusion as blood is shunted toward the body's core and they are the last to reperfuse during resuscitation (Chien et al, 2007; Poeze et al, 2005).

Based on initial human clinical trials in trauma patients, there has been an effort to integrate tissue oxygen saturation (StO_2) into the routine monitoring of critically ill patients in the ICU. Because StO_2 detects occult changes in perfusion significantly earlier than other traditional methods, it has been postulated that StO_2 may be used in goal directed resuscitation in the ICU, emergency department, and perioperative setting (Lima et al, 2009)

To date, clinical application of StO_2 in veterinary patients does not exist and prior to our recent publication (Pavlisko et al, 2014), only one study has been published in the veterinary literature. Hall and colleagues established a reference interval for StO_2 in awake dogs breathing room air and determined sites for reproducibly measuring StO_2 (Hall et al, 2008).

Chapter II: Literature Review

Oxygen Transport

Diffusion

Pulmonary ventilation is the first step in the process of oxygen transport. During inspirations, negative intra-thoracic pressure increases and atmospheric gas enters the lung. The increase in negative intra-thoracic pressure is accomplished by caudal movement of the diaphragm. During heavy breathing, the diaphragm is assisted by the intercostal muscles, which increase the thoracic diameter during the inspiratory phase. In the upper airway net movement of inspired gases is by convection up until the fourth generation of bronchi. Beyond this point the cross-sectional area increases and gas flow velocity decreases. Net gas flow from this level to the terminal alveolus is achieved by diffusion (Miller et al, 2010). Diffusion is a process by which net transfer of molecules takes place from a zone of high partial pressure to a zone of lower partial pressure. Most of the inspired gases, nitrogen for example, exist in a static equilibrium, because these gases are not extensively metabolized and rapidly reach equilibrium in the body. Oxygen on the other hand, exists in a state of dynamic equilibrium. Mitochondria consume oxygen to maintain normal physiologic function, helping to maintain a partial pressure gradient not only through the lungs, but also throughout the entire transport process (Lumb, 2010).

In the alveoli, oxygen must passively diffuse across the blood-gas barrier into the plasma where it binds to hemoglobin (Hb). The blood-gas barrier is extremely thin at 0.2 to 0.3 micrometers. The rate of diffusion across the blood-gas barrier, the diffusion capacity, is

determined by 5 factors: surface area, thickness of the membrane, pressure difference across the barrier, solubility of the gas in the tissue it has to transverse, and molecular weight of the gas (Miller et al, 2010). In the human lung, the gas-exchange surface area is exceedingly large at 50 to 100 m^2 (West, 2012). As the surface-area available for gas exchange decreases, the diffusion capacity decreases in parallel. Therefore, pulmonary blood volume is an important determinant of diffusion. As the membranes become thicker, the diffusion distance increases and the overall rate of diffusion decreases. The larger the partial pressure gradient across the blood-gas barrier, the greater the diffusion capacity. Diffusion is inversely related to the square root of the molecular weight of the gas. The larger the molecule, the more difficult it will be to pass through the membranes. Diffusion capacity is linearly related to solubility in the tissue. For example, CO_2 is almost 30 times more soluble in water than O_2 and diffuses more than 20 times faster (Miller et al, 2010).

Hemoglobin

After diffusing across the blood-gas barrier, oxygen binds to Hb contained in the red blood cells (RBC) in the pulmonary capillary network. Hb is essential to maintaining adequate oxygen delivery to the tissue and Hb bound O_2 accounts for 97% of the oxygen delivered to the tissue. Hb is a heterotetrameric compound; each monomer consists of a heme and globin. The globin is either an α or β chain that surrounds a central heme, which is a porphyrin compound coordinated to a single iron atom. The centrally located iron atom is held in place through a non-covalent bond between the iron atom and nitrogen atom in a pyrrole ring of the porphyrin compound. Each monomer has the

capacity to bind one O_2 molecule. Thus, each Hb molecule consists of 2 α and 2 β chains and has the capacity to bind 4 oxygen molecules (Boron et al, 2012).

The globin portion of the monomer is critical to the interaction between O_2 and the heme. When O_2 reacts with free ferrous iron (Fe^{2+}), it irreversibly oxidizes the Fe^{2+} to ferric iron (Fe^{3+}). In the Fe^{3+} state Hb can no longer bind oxygen. Under normal physiological conditions, the heme-O_2 interaction must be fully reversible, allowing cyclic binding and release of O_2. The interaction with the amino acids in the globin portion of the monomer cradle the heme, allowing O_2 to loosely and reversibly bind to Fe^{2+} without converting it to Fe^{3+}. When all four heme groups in the Hb molecule are devoid of O_2, Fe^{2+} shifts above the plane of its porphyrin ring by 0.06 nm distorting the porphyrin ring. In this orientation, the Fe^{2+} histidine bond is under intense stress that is transmitted throughout the Hb molecule. Locked in this tensed state (T-state), O_2 is sterically inhibited from approaching the heme and the Hb has a low affinity for O_2. As O_2 concentration begins to increase and O_2 binds to one of the Fe^{2+} atoms the Fe^{2+} begins to shift back into the plane of the porphyrin ring. As more O_2 molecules bind, a threshold is reached and the Hb reverts back into a relaxed state (R-state). In the R-state Hb affinity for O_2 increase 150 fold (Boron et al, 2012).

Elevated temperature, low pH, and high PCO_2 in the systemic capillaries of metabolically active tissue can stimulate Hb to release O_2 by acting at nonheme sites to shift the equilibrium between the T and R states of Hb toward the low-affinity T state (Boron et al, 2012). As the temperature increases there is a small shift in the pKa values of various

amino acid side chains. The change in pKa causes a shift in the net charge and the Hb-O_2 dissociation curve begins to shift to the right (Boron et al, 2012). Because Hb is an excellent H^+ buffer, it is extremely sensitive to changes in pH. During respiratory acidosis, intracellular Pco_2 increases in parallel with the extracellular Pco_2, leading to a decrease in intracellular pH and increase in the ratio of ionized Hb. In the ionized state the Hb molecule has a lower affinity for O_2. Again, resulting in a shift in the Hb-O_2 dissociation curve to the right (Boron et al, 2012). Only representative of a small portion of the Bohr effect, hypercapnia also contributes to the rightward shift of the O_2-Hb dissociation curve. As intracellular Pco_2 increases, the number of interactions between CO_2 and the unprotonated amino groups of the globulin chains increases. Formation of the negatively charged carbamino groups produces a conformational shift in the Hb, which reduces its affinity for O_2 (Boron et al, 2012). 2,3-Diphosphoglycerate, a glycolytic metabolite, alters the affinity of Hb for O_2 by binding to Hb and interacting with a central cavity formed by the β chains. Binding to Hb destabilizes the interaction between Hb and O_2, promoting the release of O_2. As Po_2 in systemic tissues decrease, glycolytic activity increases, leading to increased levels of 2,3-DPG. This decreases in O_2 affinity markedly increase O_2 release. In the pulmonary capillaries the same properties described above promote O_2 uptake (Lower temperature, PCO_2 is low, pH is high) (Boron et al, 2012).

Pulmonary Circulation

The pulmonary circulation is a low-pressure system with low vascular resistance with a pulmonary artery pressure of 20 mm Hg systolic and 8 mm Hg diastolic,. The lower

pressure can be attributed to the larger vascular diameter and shorter length of the pulmonary vessels (Miller et al, 2010). Due to the lower pressure, pulmonary capillary pressure is non-pulsatile and therefore capillary and alveolar walls can be made very thin without risking extravasation of plasma. This decreases the distance over which O_2 must diffuse and as mentioned previously decreasing the distance will facilitate diffusion. (Miller et al, 2010) This is an impressive achievement considering the flow of blood through the pulmonary circulation is approximately equal to the flow through the whole systemic circulation (Lumb, 2010). Due to the low pressure and low vascular resistance, the pulmonary circulatory system has a limited capacity to control the regional distribution of blood flow within the lungs and may be subject to the effects of gravity (Lumb, 2010).

Because the pulmonary circulation separates the right heart from the left heart, small alterations in carbon Monoxide (CO) between the two sides may result in large changes in pulmonary blood volume (Lumb, 2010). Additionally, increases in systemic vascular tone will tend to shift blood volume distribution from the systemic circulation into the pulmonary circulation. Conversely, as systemic vascular tone is diminished, pulmonary blood volume will decrease (Lumb, 2010).

The driving pressure and vascular resistance determine blood flow through the pulmonary circulation. Because the pulmonary circulation has little control over these variables, blood flow tends to be unevenly distributed throughout the lung (Miller et al, 2010). Moving from dorsal to ventral pulmonary artery pressure increase due to the

effects of increasing hydrostatic pressure. The pressure differential between the pulmonary arterial vessels in the apex and the base is approximately 11 to 15 mm Hg. As a result, there is less driving pressure to the apex than the base of the lung. The lung can be divided up into 5 zones (Miller et al, 2010). Recent evidence suggests that the pulmonary circulation may be subject to non-gravitational inhomogeneity of blood flow distribution. In a canine model, researchers demonstrated that the vertical lung blood flow distribution was nearly uniform and did not change when position was altered (Miller et al, 2010). Moreover, perfusion distribution at a given vertical level is subject to more inhomogeneity than that in the vertical direction. A greater amount of blood flow appears to be distributed to the core of the lung with less to the periphery. These observations may reflect morphologic (i.e. longer distance to the peripheral bed) and functional differences between lung vessels that determine blood flow distribution. (Miller et al, 2010)

As blood exits the pulmonary circulation and enters the left atrium the partial pressure of oxygen (PaO_2) of the blood is 95 mm Hg, this represents an admixture. Approximately 98% of the blood entering the left atrium just passed through the alveolar capillaries (PaO_2 of 104 mm Hg) and the remaining 2% of the blood has passed from the bronchial circulation. The bronchial circulation supplies oxygen and nutrients to the deep tissues of the lungs, returning deoxygenated blood to the left atrium (Hall, 2011). After exiting the heart the oxygenated blood is transported through the systemic circulation to the level of the capillary bed. In the capillaries O_2 is released from the Hb and diffuses into the tissue.

Tissue Extraction

In the peripheral tissue, as the blood enters the capillary network, the PaO_2 is still 95 mm Hg. The PaO_2 in the interstitial fluid that surrounds the cells in the peripheral tissue is 40 mm Hg. The pressure difference between these two regions causes oxygen to diffuse rapidly across the capillary wall into the interstitial tissue. As the blood exits the capillary network, the PO_2 has fallen to almost 40 mm Hg.

The intracellular PO_2 in the peripheral tissue ranges from 5 to 40 mm Hg, with a mean of 25 mm Hg. However, only a PaO_2 of 1 to 3 mm Hg is required to support normal cellular metabolism, this provides a large safety factor. The balance between DO_2 and VO_2 determines the intracellular PO_2 in the peripheral tissue. Therefore, increases in CO and CaO_2 will improve DO_2 and increase the intracellular PO_2. However, decreases in CO or CaO_2 will result in a decrease in the intracellular PO_2. Similarly, VO_2 and intracellular PaO_2 are inversely related

Microcirculation

Anatomy

The microcirculation extends from the level of the first order arteriole to the first order venule (Boron et al, 2012). As the arteries enter their target tissues they begin to divide as they course through the tissue. After approximately six to eight divisions the vessel diameter is 10 to 15 micrometers and the vessels are small enough to be called arterioles. The arterioles are surrounded by vascular smooth muscle cells that allow the vessels to alter their diameter as the smooth muscle contracts and relaxes. After an additional two

to five divisions the diameter decreases to 5 to 9 micrometers and the arterioles end and the capillary bed begins. The terminal arterioles that connect to the capillary bed are called metarterioles. The metarterioles no longer have a continuous layer of smooth muscle but instead have intermittent bands of smooth muscle that encircle the vessel at the junction between the metarterioles and the capillary. These precapillary sphincters constrict and relax, regulating blood flow through the capillary network (Hall, 2011).

Local Control of Flow Distribution

Blood flow to the tissue beds is highly variable. For example, blood flow to inactive muscles of the body is approximately 750 ml/min but during strenuous exercise blood flow can increase as high as 16,000 ml/min (Hall, 2011). Tightly regulating the distribution of flow ensures that the oxygen delivery to the tissue is adequate and the workload on the heart is kept to a minimum. Local blood flow regulation is divided into the acute control and long-term control.

During the acute control phase, changes in blood flow are achieved through vasodilation or vasoconstriction of the precapillary sphincters, the response occurs over seconds to minutes. The acute phase control is highly responsive to changes in metabolic activity. When metabolic activity is increased eight times above baseline a fourfold increase in blood flow in the region is observed (Hall, 2011). As the rate of metabolic activity increases, O_2 available to the tissue decreases and the concentration of vasodilator agents in the tissue increases. The vasodilatory compounds target the vascular smooth muscle cells in the arterioles, metarterioles, and precapillary sphincters causing vasodilation.

Vasodilator compounds including carbon dioxide (CO_2), lactic acid, adenosine, and potassium increase in response to a reduction in blood flow or an increase in cellular metabolism (Hall, 2011). It has also been speculated that a decrease in available oxygen, in tissues with high metabolic rates or low blood flows, may cause regional vasodilation. Because oxygen is required to maintain tone in the vascular smooth muscle cells it is reasonable to believe that in the absence of available oxygen the vessel will be unable to constrict (Hall, 2011).

There also appears to be an autoregulatory mechanism controlling flow distribution. When mean arterial pressure (MAP) is suddenly increased, there is initially a parallel increase in blood flow to the tissue. However, within a few minutes of the increase regional blood flow returns to baseline even if MAP remains elevated. There are two theories currently being circulated to explain this autoregulation effect. First, the metabolic theory operates under the principle that increased flow provides an excessive amount of oxygen and washes out the vasodilator compounds. As more oxygen is delivered to the tissue activity at the vascular smooth muscle cells increases closing the precapillary sphincters until the excessive O_2 is consumed. The second theory is the myogenic theory. As flow increases to the tissue the vessel diameter expands and the vascular smooth muscle cells stretch. The stretching action stimulates the cells to contract. This myogenic reflex occurs in the absence of humoral and neural influence, the response is inherent to the vascular smooth muscle cells. The precise mechanism is currently unknown (Hall, 2011). Metabolic factors can override the myogenic mechanism in tissues currently subject to a high metabolic demand.

Vasoactive substance synthesized and secreted by the endothelial cells lining the blood vessel also contribute to the acute control phase. Nitric oxide (NO), an endothelial-derived relaxing factor, is secreted in response to both chemical and physical stimuli. Once secreted NO has a short half-life, 6 seconds, so it acts locally at the site of release. In the presence of NO, guanylate cyclase activity increases in the vascular smooth muscle cells. Guanylate cyclase converts cyclic guanosine triphosphate to cyclic guanosine monophosphate and activates cyclic guanosine monophosphate-dependent protein kinase, which produces smooth muscle relaxation. Endothelin is an endothelial-derived vasoconstrictor. It is a highly potent compound that when released in nanogram quantities produces profound vasoconstriction. The stimulus for release is tissue damage, crushing or trauma to the vessel. Release helps minimize blood loss during traumatic injury and hemorrhage (Boron et al, 2012).

During the long-term control phase, changes in blood flow are achieved through alterations in number of vessels supplying the tissue or physical size of the vessel. Controlled changes manifest from days to months and provide better control of the flow distribution, meeting the needs of the tissue. Changes in vascularity are in response to increased oxygen demand and vascular endothelial growth factors (i.e. vascular endothelial growth factor, fibroblast growth factor, and angiogenin) (Boron et al, 2012). Further discussion is beyond the scope of this thesis.

Sympathetic and Parasympathetic innervation

Disseminated throughout the systemic circulatory system, sympathetic nerve fibers release norepinephrine, which binds to adrenoceptors on the vascular smooth muscle cells. As a result of adrenoreceptor activation, the majority of the vascular networks vasoconstrict, reducing blood flow to the affected tissue. Parasympathetic fibers are less abundant in vascular smooth muscle cells compared to the sympathetic nervous system. Activation of these pathways releases acetylcholine at the muscarinic receptors predominately in the glandular tissue of the body (Boron et al, 2012).

Humoral Control

Vasomotor tone also responds to humoral factors, compounds that are synthesized locally or at a distant location in glandular tissues and transported through the blood to the site of action. These compounds alter blood flow distribution to the tissue by causing vasoconstriction or vasodilation in the capillary network. Norepinephrine and epinephrine are among powerful hormones that produce mild vasoconstriction. Epinephrine and norepinephrine are both secreted by the adrenal medullae. The adrenal medullae is innervated with sympathetic nerve fibers that when activated stimulate the gland to release norepinephrine and epinephrine in the blood. These compounds travel through the systemic circulation and produce vasoconstriction by binding to the alpha-receptors in the vascular smooth muscle cells (Hall, 2011).

Angiotensin II is another powerful humoral factor that produces systemic vasoconstriction of the small arterioles. Although it will decrease the blood flow to regional tissue, it increases total peripheral resistance, increasing blood pressure.

Vasopressin or antidiuretic hormone is perhaps one of the most powerful vasoconstrictors. It is synthesized in the hypothalamus and transported down nerve axons to the posterior pituitary gland where is secreted. Although it is only released in small amounts and was thought to have little effect on vascular control, following severe hemorrhage vasopressin can increase MAP as much as 60 mm Hg (Hall, 2011).

Kinins are small polypeptides that are released in response to inflammation and produce vasodilation and increased capillary permeability. Kallikrein, a proteolytic enzyme present in the blood, is activated by maceration of the blood or tissue inflammation. Once activated, kallikrein targets alpha-2-globulins in the tissue and releases kallidin, which is converted to bradykinin by enzymes contained in the tissue. Bradykinin is rapidly inactivated by carboxypeptidase and persists for only a few minutes in the tissue (Hall, 2011).

Histamine is another local humoral vasodilatory agent found in almost every tissue within the body. Similar to bradykinin, histamine is a powerful vasodilator and increases capillary membrane permeability. Histamine is released from mast cells and basophils in damaged or inflamed tissue or in response to an allergic reaction (Hall, 2011).

Even in response to very large concentrations of vasodilatory agents blood flow is not significantly altered in most tissues. This is due to the ability of tissue to autoregulate blood flow according to the metabolic needs of the tissue. Therefore, as long as MAP is maintained at an adequate level, blood flow will be regulated according to the specific needs of the tissue (Hall, 2011).

Skeletal Muscle

Regulation of blood flow distribution in the skeletal muscle differs from other tissues in several key aspects. It begins with the external vascular supply to the skeletal muscle or the feed arteries. Approximately 30 to 50% of total vascular resistance resides in the feed arteries meaning that the most important site of blood flow control is proximal to the microvasculature (Boron et al, 2012). At rest, vascular resistance in the skeletal muscle is high and blood flow is low. As a consequence the partial pressure venous O_2 (PvO_2) is only slightly lower than the PaO_2. As O_2 demand increases during exercise and the O_2 extraction ratio (ERO_2) increases, vascular resistance in the proximal arteriole branches decreases as vasodilation ascends the resistance network. Dilation of the upstream feed arterioles is essential to increasing blood flow to the capillary network. Dilation of the vessels in the capillary network alone without dilating the proximal arterioles will resulted in limited ability to increase blood flow during strenuous exercise due to the high resistance upstream. Similar to other tissues, it is believed that metabolic byproducts (CO_2, adenosine, and K^+) trigger vasodilation. However, no single stimulus has been identified to explain this integrated response, which occurs within seconds (Boron et al, 2012).

Sympathetic nerve fibers innervate the entire vascular resistance network from the feed arteries to the level of the terminal arterioles. Release of norepinephrine from the nerve terminals results in vasoconstriction. In order to maintain adequate blood flow to the tissue, vasoconstriction is balance by the effects of local vasodilators. Regulation of blood flow in the muscle is important because skeletal muscle represents nearly one third of the total body mass and regulation of vascular tone in the muscles is essential to maintaining systemic MAP and venous return. At rest basal firing rates of the sympathetic nerves in the skeletal muscle is comparable to other systemic tissue. When the baroreceptors sense a decrease in blood pressure the rate of sympathetic firing can increase 8 to 16 fold to maintain blood pressure. The lumen of the arterioles in the skeletal muscles may completely close (Boron et al, 2012). This feature is a critical component of the homeostatic mechanisms in hemorrhagic shock. In addition to diffuse vasoconstriction, sympathetic activation also activates sympathetic-cholinergic fibers in the muscle that cause vasodilation. This response has likely evolved to enhance oxygen delivery to the muscle during the fight or flight response (Boron et al, 2012).

Hypoxia

During hypoxia, the ratio of adenosine triphosphate (ATP) to adenosine diphosphate (ADP) rapidly falls. As the cellular metabolism shifts from aerobic to anaerobic there is almost a twenty-fold reduction in the yield of ATP. Organs with lower metabolic rates are able to compensate for the decrease in ATP, but organs with high metabolic activity, the heart and brain, are unable to compensate and are at increased risk of injury. The

primary products of anaerobic metabolism are lactate and hydrogen. In most tissues, lactate diffuses out from the intracellular space into the systemic circulation where it can be quantified and used to assess the adequacy of DO_2. Because of the blood-brain barrier, it is difficult for the lactate and hydrogen ions to diffuse out of the tissue into the systemic circulation. As a result, both build up in the neurons during hypoxia producing a severe lactic acidosis. Therefor, under conditions of severe hypoxemia, it is often the profound acidosis that is responsible for the degree of dysfunction and not the deficiency in high-energy compounds. However, when the cause of hypoxia is hypoperfusion, the lactic acidosis in the CNS is not as severe because glucose must be delivered to the tissue in order to produce lactate. This is why hyperglycemic patients who experience an episode of cerebral ischemia have a higher morbidity rate then those who were normoglycemic during the hypoxic event (Lumb, 2010).

Compensatory changes during the acute phase of hypoxia are two-fold. First, ATP can be synthesized by harvesting energy released in the cleavage of high-energy phosphate bonds in phosphocreatinine. Second, adenylate kinase catalyzes the reaction between two molecules of ADP to form ATP and adenosine monophosphate (AMP). Adenine nucleotide is irreversibly lost as AMP undergoes a series of reactions to yield hypoxanthine, xanthine, uric acid, and inosine. Both of these steps slow the reduction in ATP and provide a source of energy to those tissues with high metabolic rate (Lumb, 2010).

There are a multitude of pathways contributing to cellular dysfunction during hypoxia many of which are not completely understood. Although many of these pathways are common across different tissues, the consensus is the response to hypoxia varies between tissues. Factors that contribute to the onset and severity of hypoxic injury include speed of onset, severity of hypoxia, metabolic activity, blood flow to the affected tissue and as discussed above, glucose concentration (Lumb, 2010).

In the acute phase of hypoxia there are alteration in the transmembrane potential leading to gross abnormalities in ion channel function and disruption of the ionic gradients. This leads to a hyperpolarization of the membrane and a reduction in the membrane potential and eventually spontaneous depolarization. Sodium and potassium channels are directly affected by hypoxia. Transmembrane conductance for both ions is accelerated as sodium-potassium pumps begin to fail due to a decline in ATP. Once the threshold potential is reached and the ion channels depolarize they remain locked in the open configuration and ions move freely across the membrane. In response to the falling transmembrane potential voltage gated calcium channels begin to open, rapidly increasing the intracellular calcium concentration. The increasing intracellular calcium concentration activates the ryonidine receptors leading to a release of calcium from mitochondria and endoplasmic reticulum. ATPase enzymes are activated by the increasing calcium concentration, further depleting already low ATP concentrations. Although not irreversibly damaged at this point, normal synaptic function is lost in these tissues. Glutamate and aspartate, excitatory amino acids, are released in supra-physiologic concentrations following the onset of hypoxia. As glutamate reuptake

mechanisms fail, neurotoxic levels are rapidly reached. The mechanism by which these excitatory amino acids cause damage is unknown (Lumb, 2010).

During the late phase of hypoxia, expression of several different genes are upregulated in an effort to overcome the hypoxic event. Alteration in gene expression targets four basic functions: oxygen transport, increased blood flow, increased ATP production and pH correction. Improving the O_2 carrying capacity of the blood can enhance O_2 transport to the tissue. During hypoxia there is an increase in the synthesis of erythropoietin and transferrin. Erythropoietin increases red blood cell production and transferrin increases iron transport. Synthesis of vascular endothelial growth factor (VEGF) is also increased during hypoxia. VEGF belongs to the platelet derived growth factor family and stimulates angiogenesis in an effort to restore O_2 supply to hypoxic tissue. ATP production during hypoxia is enhanced by increasing expression of genes involved in the glycolytic pathway (i.e. hexokinase, lactate dehydrogenase, pyruvate kinase and aldolase) and glucose transporter-1. Finally, pH correction occurs through upregulation of carbonic anhydrase, which buffers the metabolic acidosis (Lumb, 2010).

Monitoring Tissue oxygenation

Physiologic Rational

Oxygen delivery (DO_2) is often altered in critically ill patients, creating a state of oxygen debt and anaerobic metabolism. The severity and duration of the oxygen debt are directly linked to the development of end organ failure and death. Prompt intervention directed at reversing the underlying pathologic condition is associated with improved outcomes

whereas delayed recognition is attributed to preventable morbidity and mortality (Scott et al, 2013).

As discussed previously, during hypovolemic shock, elevated sympathetic tone produces profound vasoconstriction in the precapillary sphincters in the muscle bed, redistributing blood flow to essential organs. As a result, regional ischemia develops in the muscle. The oxygen EO_2R increases and the SvO_2 decreases as the tissue extracts increasing amount of oxygen off the Hb to maintain aerobic metabolic activity.

Near infrared spectroscopy is a non-invasive technology that monitors oxygen saturation in a peripheral skeletal muscle. Estimates of hemoglobin saturation are derived from a modified application of the Beer-Lambert law relating photon transmission to concentration of oxygenated and deoxygenated hemoglobin. Unlike pulse oximetry which measures Hb saturation on the arterial side NIRS measures Hb saturation in the microcirculation with 80% of signal acquisition coming from the venous side. Therefore, as the EO_2R increases and SvO_2 decreases during regional ischemia the StO_2 value, derived by NIRS, will decrease. The microcirculation in the peripheral skeletal muscles is the first place to manifest changes during hypovolemia making it a sentinel tissue for changes in global perfusion.

Technical Principles

At wavelengths in the red and near-infrared spectrum, 700 to 1000 nanometers (nm), biologic tissues are relatively transparent, allowing light in this spectrum to pass through

the tissue. However, propagation of light through these tissues is not absolute, but dependent on the degree of reflection, scattering and absorption by the tissue.

Light absorbing compounds, known as chromophores, results in attenuation of the signal and are present throughout biologic tissue. Predominate chromophores include melanin, myoglobin, oxyhemoglobin, deoxyhemoglobin, cytochrome aa_3, water and lipids. Each of these chromophores has a unique absorption spectra, allowing spectroscopic separation using light of different wavelengths. This means NIRS can differentiate oxygenated hemoglobin from deoxygenated hemoglobin by their light absorbance characteristics.

Light attenuation can be measured by examining changes in optical density and these changes can be quantified using the Beer-Lambert law (figure 2-1). Where A is the attenuations of light, I_O is the incident light, I is the transmitted light intensity, α is the specific extinction coefficient of the compound, c is the concentration of the absorbing compound, and d is the distance traveled by the light beam in the tissue or the path length. Thus, using this principle it is possible to measure the concentration of oxygenated Hb in a glass cuvette of known dimensions. In addition, in a solution containing multiple chromophores, with different extinction coefficients, concentrations of multiple substances can be calculated by using a different wavelength for each substance.

Figure 2-1: Beer-Lambert Equation

$$A = \text{Log}(I_O/I) = \alpha \times c \times d$$

The situation is more complicated when measuring concentrations in tissue due to the effects of scattering. Scattering occurs when light deviates from its original trajectory due to the presence of particulate matter in the path of the beam. The trajectory of the photon is determined by the size and refractive indices of the particulate and the wavelength of the light. The resulting increase in path length due to the change in trajectory results in increased absorption of light by the tissue and accounts for 80% of the total attenuation of near-infrared light. Therefore, scattering is the largest problem when attempting quantitative measurements in tissue. Only a fraction of the scattered light is detected and the loss due to scattering is unknown, making an absolute quantification of chromophore concentration not possible with the Beer-Lambert law in figure 1. However, if it is assumed that the loss due to scatter is the same for all chromophores, it is possible to solve for the concentration of chromophores. By using a differential equation between two chromophores it is possible to eliminate the unknown loss due to scatter.

Equipment

Each spectrometer consists of the same basic components, a light emitting diode, fiberoptic bundle to transmit light, tissue probe containing optodes for emission and collection, photon detection hardware, processing computer, and information display figure 2-2 (Simonson et al, 1996). The light source must be able to generate a minimum of four near-infrared wavelengths to support the algorithms that isolate the overlapping

portions of the absorption spectra for oxyhemoglobin and deoxyhemoglobin (Piantadosi et al, 1991).

Figure 2-2: Inspectra StO_2 Tissue Oxygenation System from Hutchinson Technology

The NIRS probe on the StO_2 monitors is a reflectance probe; meaning the emitting and receiving optodes are positioned in an angular arrangement on the same side. The reflectance probe interrogates a small volume of tissue and provides regional information. Because light travels in an arc with a penetration depth of approximately one-half the interoptode distance, increasing the interoptode distance augments the depth the NIRS signal travels. Therefore, the use of different probes results in the screening of different capillary beds. This is a problem considering optode distances are not standardized and vary between manufacturers. Gomez and colleagues evaluated a 15 mm and 25 mm probe and found consistently lower baseline StO_2 values with the 15 mm probe (Gomes et al, 2009)

The issue of standardization is not limited to the interoptode distance. Each manufacturer employs a different number of wavelengths and a proprietary algorithm that is proprietary and therefore unpublished. The lack of standardization of software algorithms, number of wavelengths, wavelength selection, and optode spacing confounds the ability to determine the validity of the results and may attribute to the lack of widespread acceptance (Matcher et al, 1995).

Probe Placement

There are multiple potential sites for signal acquisition in human medicine but only a few have been validated. Traditionally, the thenar eminence (the group of muscles on the palm at the base of the thumb) and forearm have been used to monitor tissue oxygen saturation. Problems associated with placement of the StO_2 probe and signal acquisition have been reported in human patients. Given the fact that fat and muscle thickness throughout the body is highly variable, different anatomical sites may potentially affect NIRS derived parameters. Darker skin pigmentation, large amounts of fat deposition, and interstitial edema have all been implicated in poor signal acquisition (Wassenarr et al, 2005; Poeze et al, 2006; Myers et al, 2005). The thenar eminence has a relatively thin layer of fat compared to other regions and minimal inter-individual variation regardless of body condition (Lipcsey et al, 2012). Furthermore, systemic edema formation is reported to have a minimal effect over the thenar eminence due to the presence of fibrous strands in its subcutaneous tissue, which limit the extent of edema formation (Poeze et al, 2006). There is minimal skin pigmentation over this region, circumventing interference caused by the presence of melanin in darker pigmented individuals.

In a study reported by Hall and colleagues (2008), they evaluated StO_2 probe placement in a canine model at four anatomic locations: lower back (epaxial muscle), forearm (digital extensor muscle), lateral thigh (biceps femoris muscle), and medial thigh (sartorius muscle). Seventy-eight healthy dogs were voluntarily enrolled in the study. Inclusion criteria consisted of weight >9 kg, normal physical examination, normal complete blood count, normal serum chemistry, systolic blood pressure ≥ 85 mm Hg, and either $SpO_2 \geq 96\%$ or $PaO_2 \geq 85$ mm Hg. Prior to application of the probe a 5 cm x 5 cm patch was shaved to minimize interference from the presence of the hair. There was no significant difference between readings obtained at the forearm, lateral thigh, and medial thigh. Readings obtained at the lower back were significantly different from the other sites. Hall and colleagues also examined the effect of body condition score on signal acquisition. They observed a significant difference in the StO_2 values obtained at the medial thigh of animals that were determined to be moderately to severely overweight. Suggesting that fat may interfere with the ability to acquire a reading at this site. They also reported that subjectively dark pigmentation seemed to interfere with the ability to obtain a reading. Based on this work the current recommendation is to place the probe over the medial thigh because of ease of positioning, limited hair, and minimal skin pigmentation (Hall et al, 2008).

Laboratory Research

Initial laboratory studies were designed to evaluate the ability of StO_2 to reflect changes in DO_2 in a hemorrhagic model. By creating a state of hemorrhagic shock in pigs Beilman and colleagues were able to significantly alter the DO_2 and demonstrate that

changes in DO_2 correspond to changes in StO_2 (Beilman et al, 1999). Subsequent animal studies have demonstrated that changes in StO_2 reflect changes in DO_2 under a variety of conditions (Crookes et al, 2004; Chaisson et al, 2003). In a hemorrhage model, Chaisson and colleagues investigated the use of a closed-loop resuscitation method in sheep. Following aortotomy, sheep were resuscitated with LRS to a normal cardiac output or a predetermined StO_2 value. Interestingly, when sheep were resuscitated to the predetermined StO_2 instead of a normal cardiac output, only half of the resuscitation volume was required to achieve full restoration of perfusion (Chaisson et al, 2003).

Clinical Research

Data from early human clinical trials with StO_2 paralleled data from the animal studies. StO_2 has shown considerable promise in assessing the severity of shock and resuscitative efforts during hemorrhagic shock. In a multi-center trial examining human patients with severe torso trauma, Cohen and colleagues demonstrated that StO_2 values obtained in the first hour of admission to the emergency department were equally reliable predictors of adverse outcome when compared to lactate and base excess. Additionally, changes in StO2 reflected changes in oxygen delivery earlier than base deficit or lactate (Putnam et al, 2007; Beilman et al, 1999).

Lima and colleagues examined the prognostic values of StO_2 in the ICU during early goal directed therapy in critically ill patients. Although they were unable to demonstrate a relationship between StO_2 and indices of global perfusion (heart rate, mean arterial pressure, continuous SvO_2) they were able to demonstrate a relationship between StO_2

and clinical abnormalities of peripheral perfusion and peripheral flow index. Furthermore, patients with low StO_2 levels at the end of the initial resuscitation effort had worse organ failure and a poorer outcome (Lima et al, 2009).

Chapter III: Hypoxemia

Introduction

Historically, when intraoperative monitoring was limited to a stethoscope and electro cardiogram, the subjective ability of the anesthesiologist to use their senses to detect subtle changes in a patient's condition was paramount to assuring a safe anesthetic episode. Over time there has been a shift to the ubiquitous application of non-invasive monitoring technologies in the perioperative setting under the pretense that more information is better, despite the absence of clinical evidence supporting this belief (Brodsky 1999; Moller et al, 1993; Orkin et al, 1993; Pedersen et al, 2009). Nevertheless, there is evidence indicating that the addition of these new monitoring technologies facilitates a more rapid detection of perioperative complications (Jayamanne et al. 1996) and that early recognition of patient deterioration has been identified as the primary determinant of the success of early intervention (Calzavacca et al. 2008).

Because organ systems are highly dependent on oxygen delivery (DO_2), perioperative monitoring has traditionally focused on oxygenation, pressure and flow. The pulmonary artery catheter (PAC) is the gold standard for assessing oxygen delivery in critically ill patients, and has historically been used to guide goal directed therapy in human medicine (Pugsley et al. 2010). Despite the additional information provided by the PAC, PACs are highly invasive, associated with a wide range of complications, not rapidly deployable, and recent evidence suggests that placement of a PAC does not improve patient outcome (Evans et al. 2009). In an effort to improve perioperative monitoring, investigators have been working to develop a noninvasive or minimally invasive hemodynamic monitor that

provide continuous, reliable assessment of oxygen delivery that is easily deployable and responds rapidly to changes in perfusion.

Near-infrared spectroscopy (NIRS) derived tissue oxygen saturation (StO_2) is one of several monitoring technologies to emerge from the effort to develop the next generation of hemodynamic monitors. Similar to pulse oximetry, StO_2 exploits the differential absorption properties of deoxygenated and oxygenated hemoglobin (Hb) to determine the ratio of oxygenated Hb to total Hb, which is reported as a percent saturation. Unlike pulse oximetry, which measures oxygen saturation in the arterial blood, StO_2 measures oxygen saturation in the vascular bed of the muscle with approximately 80% of the signal derived from the venous side of circulation. It is believed that StO_2 reflects local changes in DO_2 and oxygen consumption (VO_2) and provides a good surrogate for global tissue perfusion in human patients (Putnam et al. 2007; McKinley et al. 2000). However, the evidence in veterinary patients is very limited and in order to make this monitor useful in a clinical setting, specific data needs to be gathered directly from canine patients. Initial efforts should be aimed at establishing a relationship between DO_2 and StO_2 in canine patients under controlled conditions. DO_2 is the product of CO and CaO_2 therefore; manipulation of either of these two variables will produce a controlled change in the DO_2. Altering the CaO_2 in the laboratory setting can be accomplished by decreasing the Hb concentration through hemodilution or by decreasing the F_iO_2.

Phase one of the present study was carried out to evaluate the relationship between StO_2 and oxygen delivery index (DO_2I) in a model of hypoxemia and hyperoxemia in dogs.

We sought to test the hypothesis that tissue-specific oxygenation as measured by StO_2 would correlate with whole organism DO_2I during hypoxemia and hyperoxemia.

Materials and Methods

Animals

Eight healthy purpose-bred adult beagles were enrolled in the study. Dogs were determined to be healthy based on physical examination, complete blood cell count, and serum chemistry profile. Animals were fasted for 12 hours prior to each experiment but had unrestricted access to water. Animals were housed and cared for according to the Association for Assessment and Accreditation of Laboratory Animal Care adopted guidelines. The animal care and use committee approved this study.

Instrumentation

Following pre-oxygenation with 100% oxygen, anesthesia was induced with 5% isoflurane (Abbott, North Chicago, IL, USA) delivered by facemask. An endotracheal tube was placed and connected to a non-rebreathing system. Animals were positioned in left lateral recumbency and anesthesia was maintained with isoflurane (1.75-2.8%) in 21% oxygen and 79% nitrogen during the instrumentation period. The cephalic vein and the right dorsal pedal artery were catheterized with 20-Gauge 32 mm length over-the-needle catheters. A 5-Fr 8.5 cm hemostatic introducer (St. Jude Medical Inc, St. Paul, MN, USA) was placed in the right jugular vein. A 4-Fr x 75 cm thermodilution balloon catheter with heparin coating (Arrow International Inc, Reading, PA, USA) was advanced through the hemostatic introducer to the level of the pulmonary artery. Placement was

confirmed by identifying the pulmonary artery pressure tracing that changed to a pulmonary capillary wedge pressure tracing upon balloon inflation.

Animals were instrumented for continuous monitoring of respiratory rate (f_R), partial pressure of expired CO_2 ($P_E'CO_2$), expired fraction of isoflurane ($F_E'_{ISO}$), inspired fraction of oxygen (F_iO_2), heart rate (HR), direct systolic, mean, diastolic arterial pressures (SAP, MAP, DAP, respectively), pulmonary artery pressure (PAP), and esophageal temperature (S/5 Anesthesia monitor; GE Healthcare Datex-Ohmeda, Waukesha WI, USA). Esophageal temperature was maintained between 36° and 38°C by use of a forced-air patient warmer (Bair hugger, Arizant Inc, Eden Prairie, Minn, USA). All pressure transducers were previously calibrated with a calibration device (Delta-Cal, Utah Medical Products Inc, Midvale, Utah) then placed and zeroed at the level of the manubrium. Inspired and expired gas samples were continuously aspirated through an 8 F polypropylene catheter inserted via a side port into the endotracheal tube, with the tip positioned at the distal end of the endotracheal tube. The gas analyzer (S/5 Anesthesia monitor; GE Healthcare Datex-Ohmeda, Waukesha WI, USA) was calibrated before the experiment, with the specific calibration gas suggested by the manufacturer (Quick Cal Calibration gas, GE Healthcare, Finland). Arterial and central venous blood samples were obtained and immediately analyzed for Hb, partial pressure of oxygen in arterial blood (PaO_2), Hb saturation in arterial blood (SaO_2), pH, partial pressure of oxygen in venous blood (PvO_2), Hb saturation in venous blood (SvO_2), Base Excess (BE) and lactate (I-STAT; Abbot Point of Care Inc., East Windsor, NJ, USA). Cardiac output (CO) measurements were obtained in triplicate by thermodilution using 3 ml of iced 5%

dextrose injected into the proximal port of the Swan-Ganz catheter (SGC). The CO values were recorded as the mean of three measured values with less than 10% variation. Pulmonary artery wedge pressure (PAWP) was measured after CO determination using the SGC. Cardiac index (CI), systemic vascular resistance index (SVRI), arterial oxygen content (CaO_2), mixed venous oxygen content ($CmvO_2$), oxygen consumption (VO_2), oxygen extraction ratio (ERO_2), DO_2I and pulmonary vascular resistance index were calculated using standard formulas (Haskins et al. 2005).

Tissue oxygen saturation was determined using the InSpectra StO_2 tissue oxygenation monitor (Hutchinson Technology, Hutchinson, MN, USA). The StO_2 probe was placed over the sartorius muscle of the right leg. Prior to application of the StO_2 probe the site was shaved to minimize interference from the hair during signal acquisition. Adequate signal strength was determined by a Tissue Hemoglobin Index (THI) greater than 5. Tissue Hemoglobin Index is reported by the manufacturer to be a measure of hemoglobin present in the monitored tissue and an indicator of signal strength. In human patients THI values greater than 5 indicate sufficient hemoglobin to obtain an accurate StO_2 reading. StO_2 was continuously monitored at 2-second intervals over 1 minute and stored in the StO_2 monitor for later analysis. The StO_2 value recorded was the average value over a designated minute with a THI greater than 5.

Experimental Protocol

Following instrumentation animals were paralyzed with a loading dose of rocuronium bromide (Sandoz Canada Inc, Princeton, NJ, USA) (0.2 mg kg^{-1} IV) followed by a

constant rate infusion (1 mg kg^{-1} hr^{-1}) adjusted to facilitate ventilation. Mechanical ventilation was continued to maintain eucapnia, $P_E'CO_2$ 4.6 - 6.4 kPa (35 - 45 mm Hg). A loading dose of esmolol hydrocloride (APP Pharmaceuticals LLC, Schaumburg, IL, USA) (0.5 mg kg^{-1} IV) was administered, followed by a constant rate infusion (12 mg kg^{-1} $hour^{-1}$) adjusted to prevent hypoxia-induced tachycardia during hypoxemia. Both infusions were maintained until the end of the experimental part. A constant rate infusion of Lactated Ringer's (10 ml kg^{-1} hr^{-1}) was administered for the duration of the anesthetic period. After a 15-minute stabilization period at a F_iO_2 of 0.21 data were collected (baseline). Dogs were then evaluated under hypoxemic and hyperoxemic conditions. Order of the sequence (hypoxemic or hyperoxemic) was randomized and between each sequence dogs were subject to a 60-minute rest period at a F_iO_2 of 0.21, after which data were collected to confirm dogs had returned to baseline values (Rest). Target F_iO_2 values for each sequence were achieved by mixing nitrogen with oxygen and confirmed by the gas analyzer. In the hypoxemic sequence the F_iO_2 was initially decreased to 0.15 then to 0.10. In the hyperoxemic sequence the F_iO_2 was increased to 0.40 then to > 0.95. Data were collected at each target F_iO_2 following a 10-minute stabilization period. Upon completion of the study the F_iO_2 was increased to > 0.95 and dogs were allowed to recover. A dose of buprenorphine (Reckitt Benckiser Healthcare, Hull, England) (0.02 mg kg^{-1} IV) was administered during recovery. Dogs were monitored postoperatively until they were walking without ataxia. The following day, a physical exam was performed in all dogs and packed cell volume, total solids and blood urea nitrogen were checked.

Statistical Analysis

Main outcomes for this study were StO_2 and DO_2I. Other outcomes included $P_E'CO_2$, F_iO_2, HR, MAP, CVP, PAP, Temperature, Hb concentration, PaO_2, $PaCO_2$, pH, PvO_2, SvO_2, BE, and lactate concentration. Normal probability plots revealed that all outcomes followed a normal distribution. Subsequently, data were summarized as mean ±SD values. Effects of time period (F_iO_2 0.21 [baseline], hypoxemia F_iO_2 0.15, hypoxemia F_iO_2 0.10, hyperoxemia F_iO_2 0.40, and Hyperoxemia $F_iO_2 > 0.95$) on each outcome were assessed by use of mixed model ANOVA followed by the Tukey procedure for multiple comparisons. The linear model specified time period as a fixed effect and dog identification as the random effect. To test the association between DO_2I and StO_2 and StO_2 and SvO_2, dog-level data for DO_2I, StO_2 and SvO_2 were initially summarized (mean values) at each time period before generating Pearson correlation coefficient. Significance was set at $P < 0.05$. All analyses were performed with statistical software (SAS, version 9.2, SAS Institute Inc, Cary, NC).

Results

All 8 dogs (8 females) used in the study recovered from anesthesia without complications. They were all 2 years of age or older with a mean body weight of 8.5 ± 0.73 kg. There was no statistical difference between data collected at baseline and at the completion of the 60-minute rest period between sequences, therefore all time points were compared to baseline. Dose range for the constant rate infusions of rocuronium bromide and esmolol hydrochloride were 1 to 1.1 mg $kg^{-1}hr^{-1}$ and 12 to 15.1 mg kg^{-1} hr^{-1} respectively. Cardiopulmonary values are presented in tables 3-1, 3-2 and 3-3.

During the hypoxemic sequence, from baseline to F_iO_2 0.15 there was a significant decrease in SaO_2 but no significant change in DO_2I (458 ± 70 ml min^{-1} m^{-2} vs. 428 ± 77 ml min^{-1} m^{-2}; p = 0.97) or StO_2 (90 ± 3% vs. 88 ± 4%; p = 0.99) (Fig 3-1). As F_iO_2 was reduced to 0.10 values for SaO_2, PvO_2, SvO_2, PaO_2, CvO_2, CaO_2, THI, SpO_2, DO_2I, and StO_2 decrease significantly. These changes were accompanied by a significant increase in ERO_2, PAP, and PVRI from baseline values. Additionally, at F_iO_2 0.10, there was a 38% reduction in DO_2I (458 ± 70 ml min^{-1} m^{-2} vs. 281 ± 100 ml min^{-1} m^{-2}; p = 0.0008) and a 24% reduction in StO_2 (90 ± 3% vs. 68 ± 17%; p < 0.0001) (Fig 3-1).

During the hyperoxemic sequence, from baseline to F_iO_2 0.40, there was a significant increase in PaO_2, PvO_2, and SaO_2. These changes were accompanied by a 5% increase in DO_2I (458 ± 70 ml min^{-1} m^{-2} vs. 481 ± 122 ml min^{-1} m^{-2}; p = 0.99) and no change in StO_2 (90 ± 3% vs. 90 ± 4%; p = 0.99) (Fig 1). As F_iO_2 was increased to >0.95 there was a significant increase in PaO_2, PvO_2, SaO_2, and SvO_2 from baseline values. During this period there was a 0.6% increase in DO_2I (458 ± 70 ml min^{-1} m^{-2} vs. 461 ± 96 ml min^{-1} m^{-2}; p = 1) and a 3% increase in StO_2 (90 ± 3% vs. 93 ± 4%; p = 0.96) (Fig 3-1). There was a significant decrease in Hb at both hyperoxemic time points compared to the baseline value. Heart rate, PAP, SpO_2, CaO_2, CvO_2, ERO_2, PVRI, and THI did not change from baseline values during hyperoxemia (tables 3-1, 3-2 and 3-3).

Across all time points in the study there was no significant change in CI, SVRI, MAP, BE, Lac, VO_2. Comparison of mean DO_2I and StO_2 values across all time points yielded

a strong linear relationship, with a correlation coefficient of 0.97 ($p = 0.0009$). Comparison of mean StO_2 and SvO_2 values across all time points yield a strong linear relationship, with a correlation coefficient of 0.98 ($p = 0.0003$).

Table 3-1: Mean ± SD values for cardiovascular variables measured in 8 adult beagles during baseline and rest (F_iO_2 0.21), hypoxemia (F_iO_2 0.15 and 0.10), and hyperoxemia (F_iO_2 0.40 and >0.95). * Statistically significant difference from baseline ($P < 0.05$).

Variables	Baseline	Hypoxemia		Rest	Hyperoxemia	
	F_iO_2 0.21	F_iO_2 0.15	F_iO_2 0.10	F_iO_2 0.21	F_iO_2 0.40	F_iO_2 0.95
HR (bpm)	116 ±17	127 ±13	132 ±15	129 ±9	125 ±17	117 ±21
MAP (mm Hg)	67 ± 5	69 ± 6	70 ± 10	67 ± 4	67 ± 5	64 ± 4
CI (L min^{-1} m^{-2})	3.48 ± 0.57	3.57 ± 0.58	3.35 ± 0.91	3.28 ± 0.71	3.6 ± 0.72	3.4 ±0.74
SVRI (dynes sec $cm^{-5}m^2$)	1519 ±311	1352 ±256	1467 ±254	1294 ±284	1319 ±279	1292 ±294
Pa Mean (mm Hg)	20 ± 1	21 ± 2	27 ± 4*	20 ± 1	20 ± 1	21 ± 4
SpO_2 (%)	94 ±1	89 ±2	66 ±15*	93 ±1	95 ±0	95 ±0

Table 3-2: Mean ± SD for arterial and mixed venous blood gas values measured in the same dogs as table 3-1. * Statistically significant difference from baseline ($P < 0.05$).

Variables	Baseline	Hypoxemia		Rest	Hyperoxemia	
	F_iO_2 0.21	F_iO_2 0.15	F_iO_2 0.10	F_iO_2 0.21	F_iO_2 0.40	F_iO_2 0.95
F_iO_2	0.21 ± 0	0.14 ± 0*	0.09 ± 0.01*	0.21 ± 0	0.40 ± 0.01*	0.94 ± 0*
PaO_2 (mm Hg)	94 ± 9	62 ± 10*	32 ± 6	100 ± 11	192 ± 40*	479 ± 35*
PvO_2 (mm Hg)	49 ± 4	42 ± 3	25 ± 5*	50 ± 3	57 ± 5	70 ± 11*
SaO_2 (%)	96 ± 1	90 ± 3*	61 ± 15*	97 ± 1	99 ± 1	100 ± 0
SvO_2 (%)	81 ± 3	74 ± 4	45 ± 15*	81 ± 3	85 ± 3	90 ± 1*
BE (mmol L^{-1})	-4.75 ± 1.83	-4.88 ± 1.46	-4.75 ± 1.67	-5 ± 2.0	-4.5 ± 2.39	-2.88 ± 2.17
Hb (g dL^{-1})	10.0 ± 1.2	9.9 ± 1.1	10.2 ± 1.3	9.6 ± 1.4	9.4 ± 1.1*	9.1 ± 1.3*
Lac (mmol L^{-1})	1.58 ± 0.96	1.69 ± 0.93	1.95 ± 1.05	1.77 ± 1.05	1.54 ± 1.05	1.41 ± 1.01

Table 3-3: Mean ± SD values for calculated cardiopulmonary variables in the same dogs as table 3-1. * Statistically significant difference from baseline ($P < 0.05$).

Variables	Baseline	Hypoxemia		Rest	Hyperoxemia	
	F_iO_2 0.21	F_iO_2 0.15	F_iO_2 0.10	F_iO_2 0.21	F_iO_2 0.40	F_iO_2 0.95
CaO_2 (ml dL^{-1})	13.2 ± 1.5	12.0 ± 1.2	8.4 ± 2.0*	13.7 ± 3.3	13.3 ± 1.6	13.6 ±1.8
CvO_2 (ml dL^{-1})	11 ± 1	9 ± 1	6 ± 2*	10 ± 1	11 ± 1	11 ± 1
VO_2 (ml min^{-1})	72 ± 16	76 ± 13	67 ± 21	62 ± 21	78 ± 12	72 ± 8
ERO_2	0.15 ± 0.03	0.18 ± 0.04	0.26 ± 0.12*	0.17 ± 0.02	0.16 ± 0.02	0.16 ± 0.02
PVRI	182 ± 48	205 ± 74	280 ± 186*	165 ± 56	180 ± 55	174 ± 51
THI	15 ± 2	15 ± 2	12 ± 2*	16 ± 2	16 ± 3	16 ± 2

Fig 3-1: Mean DO_2I (squares) and StO_2 (circles) values measured in 8 adult beagles during F_iO_2 0.21 (baseline or rest), F_iO_2 0.15 and 0.10 (hypoxemia), and F_iO_2 0.40 and >0.95 (hyperoxemia). * Statistically significant difference from F_iO_2 0.21 ($P < 0.05$).

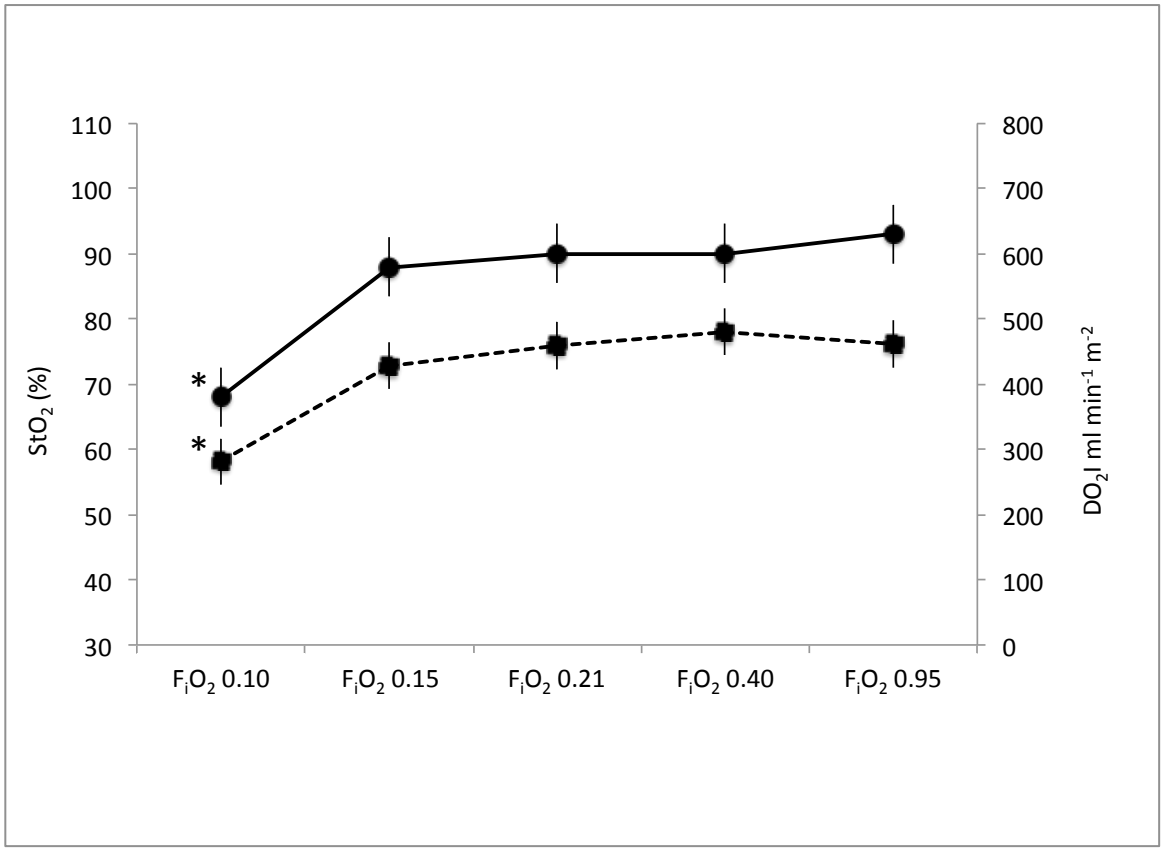

Discussion

Phase one of the present study was carried out to evaluate the relationship between StO_2 and DO_2I during hypoxemia and hyperoxemia. We sought to test the hypothesis that tissue-specific oxygenation as measured by StO_2 would correlate with whole organism DO_2I during hypoxemia and hyperoxemia. During the hypoxemic sequence there was a strong linear correlation between StO_2 and DO_2I, both achieving a statistical significance at a F_iO_2 of 0.10. Although a statistically significant difference was not observed at a

F_iO_2 of 0.15, both DO_2I and StO_2 began to trend downward as the F_iO_2 decreased below 0.21 (Fig. 3-1). The observed change in StO_2 and DO_2I during the hypoxemic sequence is most likely attributable to the decrease in CaO_2 because CI remained unchanged during the hypoxemic sequence. Bielman and colleagues (2001) reported a similar decrease in DO_2 and StO_2 following experimentally induced hypoxemia. They independently manipulated PaO_2, hemoglobin concentration and blood flow to a hind limb that had been surgically isolated from a mongrel dog. In their model, a reduction in DO_2, attributed to a reduction in CaO_2, yielded a significant decrease in StO_2 (Bielman et al, 2001).

Despite a strong linear correlation between StO_2 and DO_2I during the present study, the magnitude of change in DO_2I was larger than the change in StO_2 during the hypoxemic sequence. In a previous study, the relationship between DO_2I and StO_2 in a canine model of acute hemorrhagic shock and reperfusion was evaluated. Similar to the present study, changes in StO_2 induced by hemorrhage were not as profound as those observed in DO_2I but a strong correlation was evident between changes in StO_2 and DO_2I during hemorrhage and reperfusion (Pavlisko et al, 2014). This observation was echoed in a model of porcine hemorrhagic shock (Bielman et al, 1999). These larger fluctuations in DO_2I, compared with StO_2, may be attributable to a buffering effect in the DO_2I. There may be a critical point beyond which changes in DO_2I have little effect on StO_2 and before which changes in DO_2I significantly affect StO_2, similar to the oxygen-hemoglobin dissociation curve.

Throughout the hyperoxemia sequence there was no significant change in DO_2I or StO_2 from baseline values. Increasing the F_iO_2 beyond 0.21 had no impact on StO_2 and DO_2I because, hemoglobin had already approached maximal saturation at baseline with minimal improvement beyond a F_iO_2 of 0.21. The small increase in SaO_2 did not significantly increase CaO_2 and therefore DO_2I and StO_2. These results differ from those reported by Sullivan et al (2011). These investigators, examined the effect of nasal insufflation of supplemental oxygen on StO_2 values, measured in the inguinal region and along the surgical incision following ovariohysterectomy in dogs. They demonstrated an increase in StO_2, measured in the inguinal region (77.12 ± 1.91% vs 83.56 ± 1.91%) and 20 mm from the incision (79.11 ± 2.5 % vs 88.44 ± 2.5%), above dogs breathing room air (Sullivan et al. 2011). The explanation for the improvement in StO_2 with nasal insufflation of supplemental oxygen observed by them, can be explained by examining the PaO_2 values reported in that study. Dogs breathing room air during recovery had a mean PaO_2 of 76.91 ± 0.95 mm Hg compared to 189.77 ± 1 mm Hg in the dogs receiving oxygen supplementation. In the present study, dogs breathing room air had a PaO_2 of 94 ± 9 mm Hg at an F_iO_2 of 0.21 and therefore their Hb was maximally saturated compared to those in Sullivan's study, who were not fully saturated at an FiO_2 0.21. The reason for the lower PaO_2 observed by Sullivan et al. (2011) is likely attributed to VQ mismatch, as a result of the dogs being positioned in dorsal recumbency and not mechanically ventilated. It is also worth noting that Sullivan et al. reported much lower StO_2 values acquired in the inguinal region in their study compared to those reported here. This may be attributed to differences in technology, since they used the ODISsey tissue oximeter and StO_2 values in this study were measured with a StO_2 monitor manufactured by

Hutchinson technology. Currently, there is no standardization for monitoring tissue oxygen saturation and variation in StO_2 values has been reported between different probes (Luengo et al, 2013). Each monitor uses different wavelengths of light to determine hemoglobin saturation and the probes measure different depths into the tissue bed. The Inspectra StO_2 tissue oxygenation monitor from Hutchinson Technology measures tissue optical attenuation values at 680, 720, 760, and 800 nm and 95% of the optical signal is detected from a depth of 0 to 14 mm (Hutchinson Technology)

During the course of the study VO_2 never became linearly dependent on DO_2 and the critical DO_2 was not achieved. Failure to achieve the critical DO_2 and transition from aerobic to anaerobic metabolism was supported by the absence of change in BE and lactate. The previously reported critical DO_2 in a canine model of hypoxemia is 10-11 ml kg^{-1} min^{-1}, above which lactate production did not occur (Cilley et al, 1991). In our study the lowest value achieved during hypoxemia was 281 ml min^{-1} m^{-2} (33 ml kg^{-1} min^{-1}), significantly above the DO_2 critical reported by Cilley et al (1991). These results suggest that StO_2 may have an advantage over traditional indices of perfusion status, such as lactate and BE. Changes in BE and lactate will only manifest once DO_2 decreases below VO_2 and cellular metabolism shifts from aerobic to anaerobic. Because changes in StO_2 are observed in advance of reaching the critical DO_2, conditions producing a decrease in tissue perfusion may be corrected before lactate begins to increase and pathologic changes in the tissue begin to occur.

Measured from the pulmonary artery catheter, SvO_2 is used to determine oxygen consumption and in human medicine has been advocated as a prognostic predictor in critically ill patients because it serves as a marker of global DO_2 and VO_2 balance (Baele et al, 1982; Kasnitz et al, 1976; Edwards 1991; Rivers et al, 2001). However, pulmonary artery catheter placement is costly, highly invasive, and has inherent risk (Evans et al, 2009). Therefore, a surrogate of SvO_2, obtained non-invasively, might be of value early in the resuscitation process. In the present study there was a strong linear correlation between StO_2 and SvO_2 ($r = 0.98$; $P = 0.0003$) suggesting that StO_2 might have the same prognostic value as SvO_2. Validation studies in humans, have also demonstrated a significant correlation between NIRS derived StO_2 and SvO_2 ($r= 0.92$) (Mancini et al, 1994). However, data from human clinical research is mixed, with investigators reporting moderate to no correlation between StO_2 and SvO_2 in the clinical setting (Mulier et al, 2008; Podbregar et al, 2007). The ambiguity in this data may be attributed to the patient populations in these studies. Several of these clinical studies are reported in patients in sepsis and changes in StO_2 during sepsis are intuitively less clear. Patients in sepsis experience alterations in the microcirculation that make clinical interpretation of StO_2 data complex. Blood flow distribution during sepsis becomes highly heterogeneous due to disruption of vascular regulation caused by the presence of mediators such as cytokines and nitric oxide, as well as by microcirculatory emboli (Lam et al, 1994). These changes allow the presence of hidden hypoxic microcirculatory units next to well-perfused or even overperfused normoxic units, possibly accounting for falsely elevated StO_2 values that do not represent global oxygen delivery (Shapiro et al, 2011).

Therefore, the ability of StO_2 to estimate global oxygen delivery is highly dependent on the coupling between circulation at the probe and the central circulation.

During the hyperoxemia sequence there was a mild yet significant decrease in the Hb, which cannot be explained. Because the THI at the time of signal acquisition was >5, we can conclude there was enough Hb within the tissue to yield an accurate StO_2 value. Furthermore, in the human literature Yuruk and colleagues demonstrated that anemia in chronically anemic hematology outpatients was not associated with low StO_2 or THI levels (Yuruk et al, 2012).

Both StO_2 and SpO_2 were equally effective at detecting changes in FiO_2 in this study. Despite changing in parallel in this study, StO_2 and SpO_2 are two different technologies that measure two different variables. Unlike pulse oximetry, which measures oxygen saturation in arterial network and serves as an index of oxygenation, StO_2 measures oxygen saturation in the arterial, capillary and venous networks. Approximately 90% of StO_2 signal acquisition comes from the venous side and StO_2 reflects changes in oxygen extraction at the tissue level and serves as an index for oxygen delivery to the tissue (Hutchinson Technology). Therefore, when local tissue conditions of supply or consumption change, StO_2 will change.

In humans, the StO_2 probe is commonly placed over the thenar eminence (the muscle at the base of the thumb on the palm), but several studies have reported successful application over the deltoid muscle when the thenar eminence could not be used (i.e.

trauma to the hand). Use of these regions yields a reliable StO_2 value as determined by use of the THI. The decision to place the StO_2 probe on the medial aspect of the thigh over the sartorius muscle in this study was based on previous work by Hall et al (2008). In that study, probe placement was evaluated at 4 areas (lower region of the back, forearm, lateral aspect of the thigh, and medial aspect of the thigh) and it was determined that the medial aspect of the thigh provided the most reliable data. In the present study, the probe was placed over the right sarturious muscle (the upper leg) due to concerns that blood flow to the down extremity may be altered, but the major challenge encountered was to secure the probe to the skin and still allow good contact. We found that using surgical skin staples around the body of the probe worked well for this purpose.

There are some limitations within this study. Because all of these dogs were healthy and had no underlying disease process that would compromise oxygen delivery or alter oxygen consumption, extrapolation must be done with caution. Furthermore, the critical DO_2 was not achieved in this study. Patients were also under general anesthesia, which may have blunted the vasomotor response and blood flow redistribution in response to local hypoxemia. In addition to the effects of the anesthetic agents on vasomotor tone, the administration of esmolol may have also blunted any vasomotor response. However, because each dog in the study were on an esmolol infusion and under general anesthesia for the duration of the experiment it is unlikely the presence of these agents altered the results of the study. There were no males included in the study. Previous studies using canine models have failed to demonstrate a difference in StO_2 baseline values between males and females (Pavlisko et al, 2014; Hall et al, 2008). However, the number of

participants in these studies was low and in a larger sample population sex may have an effect on StO_2 values.

Despite becoming more commonly accepted in human medicine, several obstacles to the use of StO_2 must be overcome before this technology can gain widespread clinical application in the veterinary field. Problems associated with placement of the StO_2 probe and signal acquisition have been reported in human patients. Darker skin pigmentation, areas with large amounts of fat deposition, and interstitial edema have all been implicated in poor signal acquisition (Wassenaar et al, 2005; Poeze, 2006; Myers et al. 2005). In the present study, the dogs did not have a pigmented area in the thigh and had minimal fat deposition. However, the authors have had difficulty with signal acquisition in the clinical setting in patients with dark hair and pigmented skin, suggesting that melanin may interfere. Currently, the technology is cost prohibitive for the veterinary profession. A single use, disposable NIRS StO_2 probe is approximately $200 and the initial cost for the monitor is $15,000. There is considerable debate on how best to use this technology. Future research with StO_2 should focus on identifying specific StO_2 values that warrant intervention and what specific interventions should be performed when StO_2 values are low.

In conclusion, under the experimental conditions of hypoxemia and hyperoxemia StO_2 there was a strong correlation between StO_2 and DO_2, suggesting that StO_2 values may be used to estimate DO_2. Additionally, changes in StO_2 values preceded those in BE and

lactate concentration, indicating that StO_2 might be used as an early indicator of hypoperfusion.

Chapter IV: Hypovolemia and Resuscitation

Introduction

Oxygen is a key component in the oxidative reactions that drive cell metabolism and therefore is essential to survival. For multi-cellular organisms whose physical boundaries exceed the time-distance constraints of diffusion, circulatory systems have evolved to deliver oxygen to tissues remote to the gas exchange surface. Under normal physiologic conditions, DO_2 greatly exceeds the VO_2 in these tissues. However, during hypovolemic shock, DO_2 may become sufficiently diminished so that VO_2 becomes linearly dependent on DO_2. As a linear relationship develops between VO_2 and DO_2, oxygen delivery becomes inadequate to maintain aerobic metabolism. Timely restoration of DO_2 during hemorrhagic shock is associated with reduced morbidity and death in patients in hemorrhagic shock following traumatic injury (Pinsky et al, 2007). As a result, hemodynamic monitoring in the intensive care unit has become the cornerstone in the evaluation and treatment of the critically ill patient (Bielman et al, 1996)

Traditional non-invasive methods for indirectly monitoring oxygen delivery have focused on indices of end organ function, such as BP, urine output, and changes in mentation Porter et al, 1998). Although these methods may be effective at identifying states of profound hypoperfusion, occult hypoperfusion may go undetected in some patients, leading to poor clinical outcomes (Scalea et al, 1994; Abou-Khalil et al, 1994). Lactate and base deficit are commonly used in intensive care units to identify hypoperfusion in critically ill and injured patients. However, changes in lactate and base deficit require time to develop and do not reflect instantaneous changes in perfusion status (Crookes et

al, 2004). Additionally, lactate concentration can be falsely increased in patients with insufficient hepatic clearance (Wool et al, 1979). The advent of the pulmonary artery catheter (Swan-Ganz) has allowed for continuous monitoring of PAP and right atrial pressures in addition to CO determination, thereby allowing calculation of DO_2 in critically ill patients. Nevertheless, this technology is highly invasive, associated with a range of complications, cost prohibitive, and it is not easily deployable in an emergency (Evans et al, 2009).

Near-infrared spectroscopy has been developed out of a need for a more precise, responsive, minimally invasive method to assess tissue perfusion. Near-infrared spectroscopy exploits the differential absorption properties of deoxygenated and oxygenated Hb to determine the ratio of oxygenated Hb to total Hb in muscle. On the basis of this ratio, StO_2 is calculated and reported as a percentage. In veterinary and human clinical studies, StO_2 in muscle has proved to be a good surrogate for global tissue perfusion (Putnam et al, 2007; McKinley et al, 2000). This is likely attributable to peripheral tissues being the first to reflect hypoperfusion as blood is shunted toward the body's core and the last to reperfuse during resuscitation (Chien et al, 2007: Poeze et al, 2005).

The purpose of phase two of the study reported here was to evaluate StO_2 using NIRS in an experimental model of acute hemorrhagic shock and resuscitation in dogs. We hypothesize that tissue-specific oxygenation as measured by StO_2 will correlate with whole organism DO_2 during hemorrhagic shock and reperfusion.

Materials and Methods

Animals

Fourteen healthy purpose-bred university-owned adult Beagles were enrolled in the study. Dogs were determined to be healthy on the basis of results of physical examination, complete blood cell count, and serum biochemical profile. Food was withheld for 12 hours prior to each experiment but dogs had unrestricted access to water. Dogs were housed and cared for according to the Association for Assessment and Accreditation of Laboratory Animal Care adopted guidelines. The university animal care and use committee approved this study.

Instrumentation

Following pre-oxygenation with 100% oxygen, anesthesia was induced with 5% isoflurane[a] delivered by facemask. An endotracheal tube was placed and connected to a circle breathing system. Dogs were positioned in dorsal recumbency and anesthesia was maintained with 1.3 to 2% isoflurane in 100% oxygen during the instrumentation period. The cephalic vein and the right dorsal pedal artery were catheterized with 20-Gauge 32 mm length over-the-needle catheters. A 7-Fr 20 cm double lumen catheter[b] was placed in the left jugular vein and a 5-Fr 8.5 cm hemostatic introducer[c] was placed in the right jugular vein. Dogs were then placed in left lateral recumbency and a thermodilution balloon catheter with heparin coating[d] was advanced to the pulmonary artery. Placement was confirmed by observation of the characteristic waveform.

Dog were instrumented for continuous monitoring of respiratory rate, $ETco_2$, BIS, HR, systolic arterial blood pressure, MAP, diastolic arterial pressure, CVP, and PAP[e]. Pressure transducers were calibrated with a calibration device[f], then placed and zeroed at the level of the sternum. Bispectral index values were continuously acquired and displayed by use of a proprietary BIS module within the monitor[e]. Stainless steel subdermal needle electrodes with a 3-lead reference montage were connected to a proprietary sensor[g] and arranged as described (Henao-Guerrero et al, 2009). Briefly, the primary lead was placed on the midline over the frontal bone at the level of the zygomatic processes, the ground lead was placed rostral to the base of the left ear, and the secondary lead was placed over the temporal bone. Esophageal temperatures were continuously monitored[e] and maintained between 36° and 38°C by use of a forced-air patient warmer[h]. Arterial and mixed venous blood samples were obtained and immediately analyzed[i] for Hb, PaO_2, pH, PvO_2, BE, and lactate concentration. Cardiac output measurements were obtained in triplicate by thermodilution by use of 3 mL of iced 5% dextrose injected into the proximal port of the Swan-Ganz catheter. The CO values were recorded as the mean of 3 measured values with < 10% variation. Pulmonary artery wedge pressure was measured after CO determination with the Swan-Ganz catheter. Cardiac index, SVI, SVRI, CaO_2, $CmvO_2$, VO_2, and EO_2 were calculated with standard formulas (Haskins et al, 2005). Tissue oxygen saturation was determined with a StO_2 monitor.[j] The StO_2 probe was placed over the sartorius muscle of the left pelvic limb (dependent limb)[k]. Prior to application of the StO_2 probe, the site was shaved to minimize interference from the hair during signal acquisition. Adequate signal strength was determined by a detection of a THI > 5. Tissue Hb index is reported by the manufacturer to be a measure

of Hb present in the monitored tissue and an indicator of signal strength. In human patients, THI values > 5 indicate sufficient Hb to obtain an accurate StO_2 reading. The StO_2 was continuously monitored at 2-second intervals over 1 minute with the StO_2 monitor. The StO_2 value recorded was the mean value determined over a designated minute with a THI > 5.

Experimental Protocol

Following instrumentation, anesthesia was transitioned from isoflurane to a constant rate infusion of propofol[l], as part of an unrelated study, to facilitate mechanical ventilation with a specific ventilator. The constant rate infusion of propofol was adjusted to maintain anesthesia and BIS < 65. Dogs were paralyzed with a loading dose of rocuronium bromide[m] (0.2 mg/kg, IV) followed by a constant rate infusion (0.8 mg/kg/h) to facilitate ventilation. Mechanical ventilation[n] with 100% oxygen was continued to maintain normocapnia ($ETco_2$, 35 to 45 mmHg). Before proceeding with the experimental protocol, complete washout of isoflurane was confirmed by use of the gas analyzer[e]. Dogs were evaluated at 3 volumetric states: euvolemia, hypovolemia and hypervolemia. After a 30-minute stabilization period, euvolemic data were collected (baseline). Following this, a hypovolemic state was induced by removing blood through the double lumen catheter in the left jugular vein, until the MAP stabilized at 40 ± 5 mmHg. The blood bag collection set, containing a citrate-phosphate-dextrose-adenine solution, was suspended from a hook on the top of a vacuum chamber placed on a scale to measure total blood drawn. In preparation for autotransfusion, blood was stored in a 37 degree C incubator. Once the target MAP was achieved, dogs were maintained at a steady

hemodynamic plane for a minimum of 10-minutes before data were collected (termed hypovolemia T1). If MAP increased to a value greater than the target value, additional blood was removed until the target MAP was restored. Following restoration of the target MAP, the 10-minute equilibration period was restarted prior to data collection. Dogs were maintained in a hypovolemic state for 20 minutes and data were collected prior to resuscitation with the shed blood (termed hypovolemia T2). Shed blood was administered over 20 minutes and data were collected immediately after to confirm restoration of euvolemia (termed post-transfusion). Then hetastarch[o] was administered at 20 mL/kg over 20 minutes to achieve hypervolemia and immediately after data were collected (termed hypervolemia). Dogs were allowed to recover. A dose of buprenorphine[p] (0.02 mg/kg, IV) was administered during recovery. Dogs were monitored after surgery until they were walking without ataxia. If signs of hemorrhage were detected at the catheter sites, the dogs were transferred to the intensive care unit for 12 hours. The following day, a physical examination was performed in all dogs and PCV, total solids concentration, and blood urea nitrogen were checked. All dogs survived.

Statistical analysis

Main outcomes for this study were StO_2 and DO_2. Other outcomes included respiratory rate, $ETco_2$, HR, MAP, CVP, PAP, temperature (esophageal probe), Hb concentration, PaO_2, $PaCO_2$, pH, PvO_2, BE, and lactate concentration. Normal probability plots revealed that all outcomes followed a normal distribution. Subsequently, data were summarized as mean ± SD values. Effects of time period (normovolemia [baseline], hypovolemia with target MAP < 40 mmHg achieved and maintained steady for 10 minutes [hypovolemia

T1], then 20 minutes later [hypovolemia T2], following resuscitation with shed blood [post-transfusion] and after 20 mL/kg hetastarch [hypervolemia]) on each outcome were assessed by use of mixed model ANOVA followed by the Tukey procedure for multiple comparisons. The linear model specified time period as a fixed effect and dog identification as the random effect. To test the association between DO_2 and StO_2, dog-level data for DO_2 and StO_2 were initially summarized (by use of a mean value) at each time period before generating the Pearson correlation coefficient. Significance was set at $P < 0.05$. All analyses were performed with statistical software.[q]

Results

All 14 dogs (7 males and 7 females) used in the study recovered from anesthesia without complications. They were all 2 years of age and older, with a mean ± SD body weight of 10 ± 0.72 kg. Cardiopulmonary values were determined (Tables 4-1, 4-2 and 4-3).

Mean duration for complete isoflurane washout was 50 ± 11 minutes. Dose for the constant rate infusion of propofol ranged from 18 to 42 mg/kg/h. The time required to achieve the target MAP during hypovolemia was 26.7 ± 15.3 minutes. Blood volume removed from the dogs ranged from 297 to 519 ml, with a mean of 393.6 ± 62.3 mL. The 10-minute stabilization period had to be repeated in 6 dogs following the removal of additional blood. Following initiation of hypovolemia there was a significant increase in HR, BE, and EO_2, compared with baseline values. These changes were accompanied by a significant decrease in MAP, CVP, CI, SVI, PvO_2, and $CmvO_2$ (Tables 4-1, 4-2 and 4-3). From baseline to hypovolemia T_1, there was a 67% reduction in DO_2 (619 ± 257

mL/min/m^2 vs. 205 ± 76 ml/min/m^2; $p < 0.001$) and a 17% reduction in StO_2 (94 ± 4.4% vs. 78 ± 12.2%; $p < 0.001$ [Figure 4-1]).

Mean duration of the hypovolemic period, from hypovolemia T_1 to hypovolemia T_2, was 37.8 ± 10.9 minutes. During the hypovolemic period, there was a decrease in BE, SVRI, Hb, and CaO_2 from hypovolemia T_1 to T_2 (Tables 4-1, 4-2 and 4-3). There was no significant change in HR, MAP, CI, SVI, PvO_2, lactate concentration, and $CmvO_2$. However, there was a significant increase in lactate concentration at hypovolemia T_2, compared with the euvolemic value (Table 4-2).

Dogs received a transfusion over 20 ± 11 minutes. Upon completion of auto-transfusion of shed blood, MAP, CVP, CI, SVI, PvO_2, Hb, lactate concentration, CvO_2, and O_2 extraction returned to euvolemic values (Tables 4-1, 4-2 and 4-3). Heart rate, BE, and SVRI failed to return to euvolemic values. In comparison to hypovolemia T_2 values, StO_2 (80 ± 8.5% vs. 92 ± 6.45%; $p < 0.001$) and DO_2 (211 ± 73 mL/min/m^2 vs. 717 ± 221 mL/min/m^2; $p < 0.001$) significantly increased, returning to euvolemic values (Figure 4-1).

Subsequent to the administration of hetastarch and creation of hypervolemia, MAP, CVP, HR, CI, and PvO_2 were significantly increased, compared with euvolemic values (Tables 4-1 and 4-2). There was a significant decrease in SVRI, Hb, BE, CaO_2, and $CmvO_2$, compared with euvolemic values. No significant differences were observed with respect to SVI, lactate concentration, DO_2, StO_2, or the oxygen extraction ratio, compared with

euvolemic values. Across all time points in the study, there was no significant change in PaO_2 or VO_2. Comparison of mean DO_2 and StO_2 values across all time points yielded a strong relationship, with a correlation coefficient of 0.97 ($p = 0.005$).

Table 4-1: Mean ± SD values for cardiovascular variables measured in 14 dogs during euvolemia (Baseline), after hemorrhage (Hypovolemia T_1), 20 minutes later (Hypovolemia T_2), after transfusion (Posttransfusion), and after hetastarch administration (hypervolemia). *Significantly ($P < 0.05$) different from baseline. † Significantly ($P < 0.05$) different from hypovolemia T_1. ‡ Significantly ($P < 0.05$) different from hypovolemia T2. § Significantly ($P < 0.05$) different from Posttransfusion.

Variable	Baseline	Hypovolemia T1	Hypovolemia T2	Posttransfusion	Hypervolemia
HR (bpm)	89 ±20.29	125 ±15.79*	131 ±16.66*	127 ±9.89*	123 ±12.21*
MAP (mm Hg)	91 ±15.02	32 ±5.11*	41 ±10.82*	93 ±16.9†,‡	109 ±15.25*,†,‡,§
CI (L/min/m^2)	3.79 ±1.47	1.29 ±0.35*	1.57 ±0.49*	4.67 ±1.34†,‡	5.63 ±1.55*,†,‡
SVI (mL/beat/kg)	1.94 ±0.42	0.46 ±0.14*	0.56 ±0.21*	1.71 ±0.50	2.08 ±0.48
SVRI (dynesXsecXcm^{-5}/m^2)	2276 ±582	2290 ±682	1707 ±323*	1573 ±361*	1561 ±286*
CVP (mm Hg)	4.69 ±0.95	0.23 ±0.95*	1.07 ±0.95*	10.61 ±0.95*,†,‡	11.8 ±0.95*,†,‡

Table 4-2: Mean ± SD arterial and mixed venous blood gas values measured in the same dogs as in Table 4-1. *Significantly ($P < 0.05$) different from baseline. † Significantly ($P < 0.05$) different from hypovolemia T_1. ‡ Significantly ($P < 0.05$) different from hypovolemia T2. § Significantly ($P < 0.05$) different from Posttransfusion.

Variable	Baseline	Hypovolemia T1	Hypovolemia T2	Posttransfusion	Hypervolemia
PaO_2 (mm Hg)	475 ±39	452 ±49	450 ±51	482 ±36	471 ±36
BE (mmol/L)	-2.9 ±2.18	-6.6 ±2.06*	-8 ±2.5*,†	-7.3 ±1.73*	-5.2 ±1.72*,†,‡,§
PvO_2 (mm Hg)	75 ±21.42	37 ±6.96*	43 ±6.78*	84 ±15.44†,‡	90 ±21.10*,†,‡
Hb (g/dL)	11 ±0.97	10.74 ±1.59	9.08 ±1.34*,†	10.32 ±0.87‡	8.16 ±1.29*,†,§
Lactate (mmol/L)	0.77 ±0.52	1.06 ±0.69	1.24 ±0.76*	1.08 ±0.56	0.51 ±0.30†,‡,§

Table 4-3: Mean ± SD values for cardiopulmonary variables calculated in the same dogs as in Table 4-1. *Significantly ($P < 0.05$) different from baseline. † Significantly ($P < 0.05$) different from hypovolemia T_1. ‡ Significantly ($P < 0.05$) different from hypovolemia T2. § Significantly ($P < 0.05$) different from Posttransfusion.

Variable	Baseline	Hypovolemia T1	Hypovolemia T2	Posttransfusion	Hypervolemia
CaO_2 (mL/dL)	16.17 ±1.33	15.74 ±2.17	13.52 ±1.84*	15.23 ±1.14‡	12.35 ±1.69*,†,§
$CmvO_2$ (mL/dL)	13.70 ±1.48	8.29 ±2.25*	7.83 ±1.95*	12.97 ±1.29†,‡	10.54 ±1.62*,†,‡,§
VO_2 (mL/min/m^2)	89.08 ±29.79	94.43 ±41.49	84.22 ±17.30	104.56 ±21.64	98.75 ±21.59
EO_2 (%)	0.15 ±0.04	0.47 ±0.12*	0.42 ±0.10*	0.15 ±0.03†,‡	0.15 ±0.03†,‡
THI	16 ±2.91	14 ±2.18*	14 ±2.40*	16 ±2.34†,‡	15 ±2.90†,‡

Figure 4-1: Mean DO_2I (squares) and StO_2 (diamonds) values at euvolemia (baseline), after hemorrhage (Hypovolemia T_1), 20 minutes later (Hypovolemia T_2), after transfusion (Post-transfusion), and after hetastarch administration (Hypervolemia) in 14 dogs. *Significantly ($P < 0.05$) different from baseline. † Significantly ($P < 0.05$) different from hypovolemia T1. ‡ Significantly ($P < 0.05$) different from hypovolemia T2.

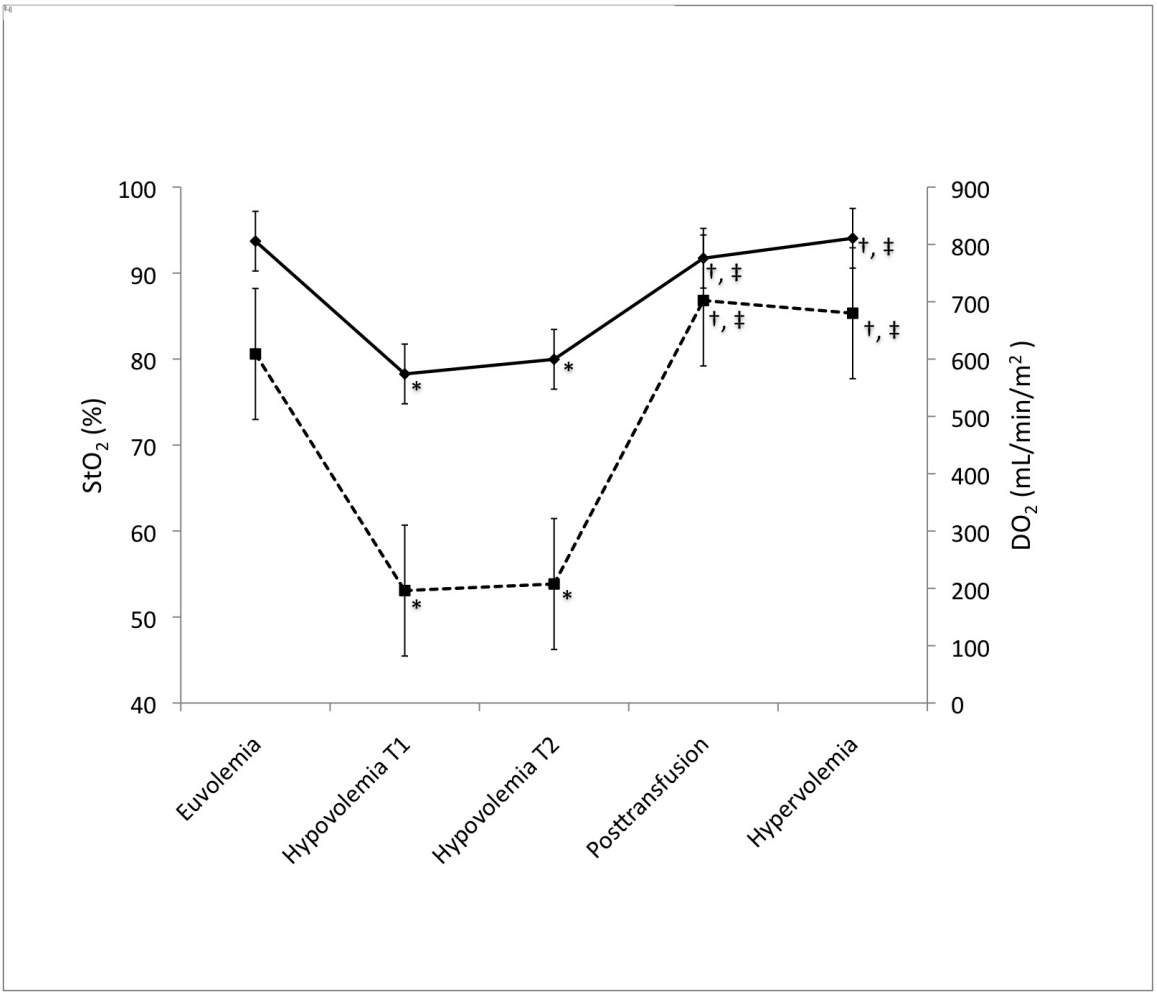

Discussion

Phase two of the present study was carried out to evaluate StO_2 using NIRS in an experimental model of acute hemorrhagic shock and resuscitation in dogs. We sought to test the hypothesis that tissue-specific oxygenation as measured by StO_2 would correlate with whole organism DO_2 during hemorrhagic shock and reperfusion.

Following induction of hemorrhage shock, there was a significant decrease in DO_2 and StO_2. Although the decrease in DO_2 was greater than the decrease in StO_2, the data revealed a strong correlation between StO_2 and DO_2 during the period between baseline and hypovolemia T_1. As dogs received the autotransfusion, leading to the restoration of euvolemia, StO_2 and DO_2 significantly increased toward baseline values and a strong correlation was again observed between StO_2 and DO_2. These results are similar to those obtained in previous studies in other species. McKinley et al monitored StO_2 values during resuscitation and for the first 24 hours following admission of human patients that sustained severe abdominal trauma; StO_2 correlated with changes in DO_2 and was useful in guiding resuscitation in severely injured trauma patients (McKinley et al, 2000). In a study of the relationship between DO_2 and StO_2 during experimental acute hemorrhagic shock in splenectomized pigs, a target blood volume of 28% was removed (Beilman et al, 1999). Similar to the present study, changes in StO_2 induced by hemorrhage were not as profound as those observed in DO_2 and a strong correlation was evident between changes in StO_2 and DO_2 during hemorrhage and reperfusion. The larger fluctuation in DO_2, compared with StO_2, may be attributable to a buffering effect in the DO_2. There may be a critical point beyond which changes in DO_2 have little effect on StO_2 and before which

changes in DO_2 significantly affect StO_2, similar to the oxygen-hemoglobin dissociation curve.

Changes in BE and lactate concentration, the traditional markers of perfusion, lagged behind changes in DO_2 and StO_2 following the induction of hemorrhagic shock and were slower to return to baseline following fluid resuscitation. This finding was in accordance with clinical and laboratory studies, in which changes in StO_2 precede changes in lactate concentration and base deficit (Bielman et al, 1999; Crookes et al, 2004). Following induction of hemorrhagic shock, statistical analysis indicated that the increase in lactate concentration was significant, but the increase was not of sufficient magnitude to be considered clinically important. This can be explained by the fact that EO_2 was increased in an attempt to maintain aerobic metabolism and the body reserves were not exhausted; therefore, critical DO_2 was not achieved. Additionally, VO_2 did not change linearly with DO_2, as would be expected after an anaerobic threshold is reached. Conversely, the StO_2 monitor detected changes in regional tissue perfusion before changes in lactate concentration and BE occurred, suggesting that StO_2 may be a valuable tool in identifying patients in the initial stage of shock before critical changes in cellular metabolism occur.

Presently, the effects of volume overload on NIRS acquired StO_2 are unknown. It has been speculated that volume overload may alter the reflectance by creating scatter, leading to falsely decreased StO_2 values (Rhee et al, 1997). In the present study, hypervolemia had no effect on StO_2 or DO_2. However, the dogs in this study were not

subject to extreme fluid overload and time was not allowed for fluid shift to occur. As fluid moves into the interstitial space, altering tissue density, the potential exists to affect the reflectance by creating scatter or decreasing tissue penetration by the near-infrared light. The data obtained in this study indicated that StO_2 would not be an effective tool for assessing fluid overload. Additional studies are indicated to determine how fluid overload affects StO_2 over time.

Tissue hemoglobin index is an indicator of signal strength reported by the StO_2 monitor and it is reported as a number in the range of 1 to 99. The THI corresponds to the amount of hemoglobin present in the monitored tissue. A THI > 5.0 indicates sufficient hemoglobin for the monitor to obtain a reliable StO_2 value in human patients under most circumstances (Huychinson Technology Inc, 2013). The relationship between THI and signal accuracy has not been verified in dogs and on the basis of clinical experience we believe values need to be > 5.0 to indicate a reliable signal. The THI values in this study were all > 5.0. Presently, the usefulness of THI is still under investigation but in the present study changes in THI values were similar to those in DO_2 and StO_2 values across all volemic states. These changes were probably caused by extra-vascular and vascular hemoglobin concentrations resulting from changes in the volume of the underlying vascular bed, as occur during hemorrhage and reperfusion.

It is important to distinguish the difference between StO_2 measurements and another commonly used oxygen measurement provided by pulse oximetry, SpO_2. Unlike pulse oximetry, which measures oxygen saturation in arterial blood, StO_2 measures oxygen

saturation in the vascular bed of the muscle. Although pulse oximetry reflects changes in oxygenation, StO_2 reflects changes in use of oxygen at the tissue level. Therefore, when local tissue conditions of supply and consumption change, StO_2 will change but SpO_2 will not. This would be a typical finding in a patient with adequate ventilation but poor oxygen delivery from causes such as poor CO, anemia, or hypovolemia. In the present study, there were no changes in SpO_2 with changes in volemic states (data not shown).

Problems associated with placement of the StO_2 probe and signal acquisition have been reported in human patients. Darker skin pigmentation, areas with large amounts of fat deposition, and interstitial edema have all been implicated in poor signal acquisition (Wassenarr et al, 2005; Poeze et al 2006; Myers et al 2005). In humans, the StO_2 probe is placed over the deltoid muscle or more commonly the thenar eminence (the group of muscles on the palm at the base of the thumb). Use of these regions yields a reliable StO_2 value as determined by use of the THI. The decision to place the StO_2 probe on the medial aspect of the thigh over the sartorius muscle in this study was based on previous work by Hall et al (Hall et al, 2008). In that study, probe placement was evaluated at 4 areas (lower region of the back, forearm, lateral aspect of the thigh, and medial aspect of the thigh) and it was determined that the medial aspect of the thigh provided the most reliable data. In the present study, the dogs did not have a pigmented area in the thigh and had minimal fat deposition. However, the authors have had difficulty with signal acquisition in the clinical setting in patients with dark hair and pigmented skin, suggesting that melanin may interfere. In the present study, the major challenge was to

secure the probe to the skin and still allow good contact. We found that using surgical skin staples around the body of the probe worked well for this purpose.

Phase two had several limitations. Blood was removed through an intravascular catheter instead of creating a surgical lesion. Although this methodology allows for standardization among animals, it does not completely reflect the clinical situation and this factor has to be considered when interpreting the results. Furthermore, the study was conducted while dogs received general anesthesia with a fractional inspired oxygen concentration of 0.95, and resuscitation of trauma patients in the emergency room may occur at lower oxygen concentrations, leading to an inability of DO_2 to meet oxygen demands and therefore a faster onset of a state of shock.

Additionally, these dogs were not splenectomized, which accounted for the variability in the time to achieve target MAP and total blood volume removed. Six of the dogs required removal of additional blood after compensation, which was characterized by tachycardia and increase in MAP. Despite the variability attributed to the presence of a spleen in these dogs, this condition more closely resembles a clinical scenario and allows for better extrapolation of the data.

Despite becoming more commonly accepted in human medicine, several obstacles to the use of StO_2 must be overcome before this technology can gain widespread clinical application in the veterinary field. The technology is cost prohibitive for the veterinary profession with the cost of a single-use, disposable StO_2 probe at approximately $200 US.

There is considerable debate on how best to use this technology. Presently, we do not know what specific StO_2 values warrant interventions and what specific interventions should be performed when StO_2 values are low. However, under the experimental conditions of hemorrhagic shock and resuscitation in the study reported here, there was a strong correlation between StO_2 and DO_2, suggesting that StO_2 values may be used to estimate DO_2 values. Additionally, changes in StO_2 values preceded those in BE and lactate concentration, indicating that StO_2 might be used as an early indicator of hypoperfusion.

References:

Abou-Khalil B, Scalea TM, Trooskin SZ, et al. Hemodynamic response to shock in young trauma patients: need for invasive monitoring. Crit Care Med 1994; 22: 633-9.

Barach P, Small SD. Reporting and preventing medical mishaps: lessons from non-medical near miss reporting systems. BMJ 2000; 320(7237): 759-763.

Baele PL, McMichan JC, Marsh HM, et al. Continuous monitoring of mixed venous oxygen saturation in critically ill patients. Anesth Analg 1982; 61: 513-517.

Bielman GJ, Cerra FB. The future. Monitoring cellular energetics. Crit Care Clin 1996;12(4):1031–1042.

Beilman G, Groehler K, Lazaron V, et al. Near-Infrared spectroscopy measurement of regional tissue oxyhemoglobin saturation during hemorrhagic shock. Shock 1999; 12(3): 196-200

Beilman GJ, Myers D, Cerra FB et al. Near-infrared and nuclear magnetic resonance spectroscopic assessment of tissue energetics in an isolated, perfused canine hind limb model of dysoxia. Shock 2001; 15(5): 392-397.

Boron W and Boulpaep E. Medical Physiology A Cellular and Molecular Approach. Philadelphia: Elsevier, 2012. Print.

Brodsky JB. What intraoperative monitoring makes sense? Chest 1999; 115(5S): 101s-105s.

Cain S. Oxygen delivery and uptake in dogs during anemic and hypoxic hypoxia. J Appl Physiol Respir Environ Exerc Physiol 1977; 42(2): 228-234.

Calzavacca P, Licari E, Tee A, et al. A prospective study of factors influencing the outcome of patients after medical emergency team review. Intensive Care Med 2008; 34(11): 2112-2116.

Chaisson N, Kirschner R, Deyo D, et al. Near-Infrared Spectroscopy-guided Closed-Loop Resuscitation of Hemorrhage. J of Trauma 2003; 54(5): 183-192.

Chien LC, Lu KJ, Wo CC, Shoemaker WC. Hemodynamic patterns preceding circulatory deterioration and death after trauma. J Trauma 2007; 62: 928-932.

Cilley R, Scharenberg A, Bongiorno P. Low oxygen delivery produced by anemia, hypoxia, and low cardiac output. J Surg Res 1991; 51: 425-433

Crookes B, Cohn S, Burton E, et al. Noninvasive muscle oxygenation to guide fluid resuscitation after traumatic shock. Surgery 2004; 135: 662-670.

Edwards JD. Oxygen transport in cardiogenic and septic shock. Crit Care Med 1991; 19: 658-663.

Evans D, Doraiswamy V, Prosciak M, et al. Complications associated with pulmonary artery catheters: a comprehensive clinical review. Scan J of Surgery 2009; 98: 199-208.

Hall J. Guyton and Hall Textbook of Medical Physiology. Philadelphia: Elsevier, 2011. Print.

Hall K, Powell L, Beilman G, et al. Measurement of tissue oxygen saturation levels using portable near-infrared spectroscopy in clinically healthy dogs. J Vet Emerg Crit Care. 2008: 18(6); 594-600

Haskins S, Pascoe P, Ilkiw J et al. Reference cardiopulmonary values in normal dogs. Comp Med 2005; 55: 156-161.

Henao-Guerrero PN, McMurphy R, Kukanich B, et al. Effect of morphine on the bispectral index during isoflurane anesthesia in dogs. Vet Anaesth Analg 2009; 36:133–143.

Hutchison Technology Inc. Web Site. Tissue oxygen monitor. Available at: http://www.htibiomeasurement.com. Accessed March 2013.

Jayamanne DG, Gillie RF. The effectiveness of perioperative cardiac monitoring and pulse oximetry. Eye 1996; 10: 130-132.

Kasnitz P, Druger GL, Zorra F, et al. Mixed venous oxy- gen tension and hyperlactemia. Survival in severe cardiopulmonary disease. JAMA 1976; 236: 570-574.

Lima A, Bommel J, Jansen T, et al. Low tissue oxygen saturation at the end of earl goal-directed therapy is associated with worse outcome in critically ill patients. Crit Care 2009 (ePub); 13(s5).

Luengo C, Resche-Rigon M, Damoisel C, et al. Comparison of two different generations of NIRS devices and transducers in healthy volunteers and ICU patients. J Clin Monit Comput 2013; 27(1): 71-79.

Lumb A. Nunn's Applied Respiratory Physiology 7th Ed. Philadelphia: Elsevier, 2010. Print.

Mancini DM, Bolinger L, Li H, Kendrick K et al. Validation of near-infrared spectroscopy in humans. Journal of Applied physiology 1994; 77(6): 2740-7.

McKinley B, Marvin R, Cocanour C, et al. Tissue hemoglobin O_2 saturation during resuscitation of traumatic shock monitored using near infrared spectroscopy. J Trauma 2000; 48(4): 637-642

Mesquida J, Masip J, Gili G et al. Thenar oxygen saturation measured by near infrared spectroscopy as a noninvasive predictor of low central venous oxygen saturation in septic patients. Intensive Care Med 2009; 35: 1106-1109.

Miller R, Eriksson L, Fleisher L, et al. Miller's Anesthesia 7th Ed. Philadelphia: Elsevier, 2010. Print.

Moller JT, Johannessen NW, Espersen K, et al. Randomized evaluation of pulse oximetry in 20,802 patients; II: perioperative events and postoperative complications. Anesthesiology 1993; 78: 445-453.

Mulier KE, Skarda DE, Taylor JH, et al. Near-infrared spectroscopy in patients with severe sepsis: correlation with invasive hemodynamic measurements. Surg Infect 2008; 9: 515-519.

Myers DE, Anderson LD, Seifert RP, et al. Noninvasive method for measuring local hemoglobin oxygen saturation in tissue using wide gap second derivative near-infrared spectroscopy. J Biomed Opt 2005; M 10:034017.

Orkin FK, Cohen MM, Duncan PG. The quest for meaningful outcomes. Anesthesiology 1993; 78(3): 417-422.

Pavlisko ND, Henao-Guerrero N, Killos MB, et al. Evaluation of tissue oxygen saturation with near-infrared spectroscopy during experimental acute hemorrhagic shock and resuscitation in dogs. Am J Vet Res 2014; 75(1): 48-53.

Pedersen T, Moller AM, Hovhannisyan K. Pulse oximetry for perioperative monitoring. Cochrane Database 2009; Syst Rev 4: CD002013.

Pinsky M. Hemodynamic evaluation and monitoring in the ICU. Chest 2007; 132: 2020-2029

Podbregar M, Mozina H. Skeletal muscle oxygen saturation does not estimate mixed venous oxygen saturation in patients with severe left heart failure and additional severe sepsis or septic shock. Crit Care 2007; 11:R6.

Poeze M, Solberg BC, Grave JW, et al. Monitoring global volume-related hemodynamic or regional variables after initial resuscitation: What is a better predictor of outcome in critically ill septic patients? Crit Care Med 2005; 33: 2494-2500.

Poeze M. Tissue-oxygenation assessment using near-infrared spectroscopy during severe sepsis: confounding effects of tissue edema on StO_2 values. Intensive Care Med

2006; 32: 788–789.

Porter JM, Ivatury RR. In search of the optimal endpoints of resuscitation in trauma patients: a review. J Trauma 1998; 44: 908–914.

Pugsley J, Lerner AB. Cardiac output monitoring: is there a gold standard and how do the newer technologies compare? Semin Cardiothorac Vasc Anesth 2010; 14 (4): 274-282.

Putnam B, Bricker S, Fedorka P, et al. The correlation of near-infrared spectroscopy with changes in oxygen delivery in a controlled model of altered perfusion. Am Surg 2007; 10: 1017-1022.

Rhee P, Langdale L, Mock C, et al. Near-infrared spectroscopy: continuous measurement of cytochrome oxidation during hemorrhagic shock. Crit Care Med 1997; 25: 166–170.

Rivers E, Nguyen B, Havstad S, et al. Early goal-directed therapy in the treatment of severe sepsis and septic shock. N Engl J Med 2001; 345,:1368-1377.

Scalea TM, Maltz S, Yelon J. et al. Resuscitation of multiple trauma and head injury: role of crystalloid fluids and inotropes. Crit Care Med 1994; 20: 1610-5

Sullivan LA, Campbell VL, Radecki S, et al. Comparison of tissue oxygen saturation in ovariohysterectomized dogs recovering on room air versus nasal oxygen insufflation. J Vet Emerg Crit Care 2011; 21(6): 633-638.

Wassenaar EB, Van den Brand JG. Reliability of near-infrared spectroscopy in people with dark skin pigmentation. J Clin Monit Comput 2005: 19; 195-199.

West J. Respiratory Physiology 9th Ed. Philadelphia: Lippincott Williams and Wilkins 2012. Print.

Wool PJ, Record CO. Lactate elimination in man: effects of lactate concentration and hepatic dysfunction. Eur J Clin Invest 1979; 9: 397-404.